

1 CropSuite v1.0 - A comprehensive open-source crop 2 suitability model considering climate variability for 3 climate impact assessment

4 F. Zabel¹, M. Knüttel¹, B. Poschlod²

5 ¹Department of Environmental Sciences, University of Basel, 4056 Basel, Switzerland

6 ²Center for Earth System Research and Sustainability, Universität Hamburg, 20144 Hamburg, Germany

7

8 *Correspondence to:* florian.zabel@unibas.ch

9

10 **Abstract.**

11 Increasing demand for agricultural land resources and changing climate conditions require for strategic land-use planning
12 and the development of adaptation strategies. Therefore, information about the suitability of agricultural land is a
13 prerequisite. Current suitability approaches often focus on single crops, can only be applied regionally and usually neglect
14 the impact of climate variability on crop suitability. Here, we introduce CropSuite, a new comprehensive and easy-to-use
15 crop suitability model that allows to overcome these shortcomings. It provides a graphical user interface (GUI) and a
16 wide range of pre- and postprocessing options, including a tool for data analysis, which allows users to easily apply the
17 model and analyze the results. Further, it includes a spatial downscaling approach for climate data, which enables crop
18 suitability analysis at very high spatial resolution. CropSuite uses a fuzzy logic approach and is based on the assumption
19 of Liebig's law of the minimum. An expandable number of environmental and socio-economic factors that impact on
20 crop suitability can flexibly be integrated into CropSuite by determining membership functions. CropSuite allows for the
21 consideration of irrigated and rainfed agricultural systems, vernalization requirements for winter crops, lethal temperature
22 thresholds, photoperiodic sensitivity and several other limitations for crop growth. The model endogenously calculates
23 and outputs climate-, soil-, and crop suitability, the optimal sowing- and harvest dates, the potential for multiple cropping,
24 the (most) limiting factor(s), as well as the recurrence rate of potential crop failures according to the inter-annual climate
25 variability.

26 In this study, we apply CropSuite for 48 crops at a spatial resolution of 30 arc seconds (1 km at the equator) for Africa.
27 Thereby, we consider regionally important staple and cash crops that are usually understudied, such as coffee, cassava,
28 banana, oil palm, cocoa, cowpea, groundnuts, mango, millet, papaya, rubber, sesame, sorghum, sugar cane, tobacco, and
29 yams. We find that the consideration of climate variability for calculating crop suitability makes a significant difference
30 on suitable areas, but also affects optimal sowing dates, and multiple cropping potentials. The most vulnerable regions

31 for climate variability are identified in Somalia, Kenya, Ethiopia, South Africa, and the Maghreb countries. The results
32 provide valuable crop-specific information that can be further used for climate impact assessments, adaptation and land-
33 use planning at global, regional, or local scale. CropSuite is provided open source and could be of interest for model
34 developers, scientists, and a wide range of potential users and stakeholders, such as farmers, companies, GOs, and NGOs.

35

36 **Key Words: Agriculture, Africa, Optimal Sowing Dates, Multiple Cropping, Maize**

37 **1 Introduction**

38 Climate change poses major challenges for agricultural production and food security. With warming climate, agricultural
39 suitability changes and suitable areas shift towards higher latitudes (Franke et al., 2021; Zabel et al., 2014). Crop
40 suitability models allow for a quantitative evaluation of land for crop cultivation and can therefore assess how the
41 suitability of land changes with changing climate. Contrary to mechanistic crop models (Jägermeyr et al., 2021;
42 Jägermeyr et al., 2020; Müller et al., 2024), crop suitability models are based on empirical approaches but are less
43 computational intensive and thus allow for the consideration of more crops at higher spatial resolution (Zabel et al., 2014).
44 As a result, crop suitability models provide important insights for sustainable land-use planning and climate change
45 adaptation, e.g. through cultivar change or land-use change. Akpoti et al. (2019) give an overview of existing crop
46 suitability approaches. Most studies are applied at regional scale (Maleki et al., 2017; Bonfante et al., 2015; Ranjitkar et
47 al., 2016), while just a few global approaches exist (Akpoti et al., 2019). In addition, most studies focus just on single
48 crops and do not cover a variety of different crops (Ramirez-Villegas et al., 2013; Akpoti et al., 2020). Particularly for
49 Africa, domestically consumed staple crops, such as yams and cassava are often overseen in current studies, due to minor
50 economic relevance, despite their regional importance for food security (Chapman et al., 2020; Chemura et al., 2024;
51 Van Zonneveld et al., 2023; Karl et al., 2024). So far, none of the existing approaches systematically considers the impact
52 of climate variability on crop suitability, which is a major shortcoming, since climate variability is expected to increase
53 with climate warming and has a strong impact on agriculture (Vogel et al., 2019; Goulart et al., 2021; Ipcc, 2021).

54 The aim of this study is to introduce the CropSuite model, which is based on the crop suitability approach developed by
55 Zabel et al. (2014) and has continuously been further developed by Cronin et al. (2020) and Schneider et al. (2022a). The
56 model has previously been applied globally for 23 crops for different climate scenarios (Zabel, 2022). The model applies
57 Liebig's law of the minimum, assuming that the scarcest resource limits the crop growth. CropSuite is based on a fuzzy
58 logic approach where, in contrast to Boolean logic, the truth value of variables can be any real number between 0 and 1.
59 In fuzzy logic, fuzzy sets consist of elements whose degrees of memberships are described by membership functions
60 (Zadeh L.A., 1965). In our approach, we apply fuzzy logic to create crop-specific membership functions (Fig. 1)
61 describing the abiotic crop requirements between 0 (not suitable) and 100 (highly suitable) according to various climatic,
62 soil, and topographic variables (Zabel et al., 2014). Using a value range between 0 and 100 (instead of 0 and 1) enables

63 the use of an 8-bit integer data type for the internal calculation and storage of the results, which allows efficient use of
64 memory and hard disk. This approach is adopted, fundamentally redesigned and expanded with the goal to provide a
65 comprehensive but easy-to-use and flexible open-source model that can be applied e.g. by scientists, farmers, companies,
66 national or international GOs, and NGOs. Therefore, CropSuite is now completely reprogrammed in Python and consists
67 of a graphical user interface (GUI), as well as several pre-processing and analysis tools, e.g. for selecting a simulation
68 domain, statistically downscaling the climate data, interpolating the membership functions and automatically analyzing
69 and mapping the results. In addition, CropSuite is complemented with a new approach to consider the impact of climate
70 variability on crop suitability. It includes a user manual, which is provided together with the source code (Knüttel and
71 Zabel, 2024).

72 2 Methods and Data

73 For this study, we apply CropSuite for Africa at 30 arc seconds spatial resolution (approximately 1 km² at the equator)
74 with the goal to simulate relevant but often overseen crops for this continent (Van Zonneveld et al., 2023). Table 1 shows
75 the 48 crops, that have been parameterized and simulated with CropSuite.

76
77 **Table 1: List of 48 considered crops simulated with CropSuite.** Binomial names are given in brackets.

1. Alfalfa (<i>Medicago sativa</i>)	25. Olive (<i>Olea europacae</i>)
2. Arabica Coffee (<i>Coffea arabica</i>)	26. Onion (<i>Allium cepa</i>)
3. Avocado (<i>Persea americana</i>)	27. Papaya (<i>Carica papaya</i>)
4. Banana (<i>Musa spp.</i>)	28. Pea (<i>Pisum sativum</i>)
5. Barley (<i>Hordeum vulgare</i>)	29. Pineapple (<i>Ananas comosus</i>)
6. Beans (<i>Phaseolus vulgaris</i>)	30. Potato (<i>Solanum tuberosum</i>)
7. Cabbage (<i>Brassica oleracca</i>)	31. Rapeseed (<i>Brassica napus</i>)
8. Carrot (<i>Daucus carota</i>)	32. Rice (<i>Oryza sativa</i>)
9. Cashew (<i>Anacardium occidentale</i>)	33. Robusta Coffee (<i>Coffea canephora</i>)
10. Cassava (<i>Manihot esculenta</i>)	34. Rubber (<i>Hevea brasiliensis</i>)
11. Castor Bean (<i>Ricinus communis</i>)	35. Rye (<i>Secale cereale</i>)
12. Chickpea (<i>Cicer arietinum</i>)	36. Safflower (<i>Carthamus tinctorius</i>)
13. Citrus (<i>Citrus spp.</i>)	37. Sesame (<i>Sesamum indicum</i>)
14. Cocoa (<i>Theobroma cacao</i>)	38. Sorghum (<i>Sorghum bicolor</i>)
15. Coconut (<i>Cocos nucifera</i>)	39. Soy (<i>Glycine maximum</i>)
16. Cotton (<i>Gossypium hirsutum</i>)	40. Sugar Cane (<i>Saccharum officinarum</i>)
17. Cowpea (<i>Vigna unguiculata</i>)	41. Sunflower (<i>Helianthus annuus</i>)
18. Green Pepper (<i>Capsium annuum</i>)	42. Sweet Potato (<i>Ipomoea batatas</i>)
19. Groundnut (<i>Arachis hypogaea</i>)	43. Tea (<i>Camellia sinensis</i>)
20. Guava (<i>Psidium guajava</i>)	44. Tobacco (<i>Nicotiana tabacum</i>)
21. Maize (<i>Zea mais</i>)	45. Tomato (<i>Solanum lycopersicum esculentum</i>)
22. Mango (<i>Mangifera indica</i>)	46. Watermelon (<i>Colocynthis citrullus</i>)

23. Millet (<i>Pennisetum americanum</i>)	47. Wheat (<i>Triticum aestivum</i>)
24. Oil Palm (<i>Elaeis guineensis</i>)	48. Yams (<i>Dioscorea</i>)

78
79
80
81
82
83
84
85
86
87
88
89
90
91
92
93
94
95
96
97
98
99
100
101
102
103
104
105
106
107

We simulate a 20-year time period from 1991 to 2010 using the Climate Hazards group Infrared Precipitation with Stations (CHIRPS) v2.0 daily data for precipitation (Funk et al., 2015) and the Climate Hazards Center Infrared Temperature with Stations (CHIRTS) v1.0 data for temperature (Funk et al., 2019; Verdin et al., 2020) at 2.5 arc minutes spatial resolution for Africa. Both data sets provide climatologies at daily to monthly resolution based on a combination of satellite remote sensing and climate stations. They benefit from long-term geostationary satellite observations, delivering consistent data since the 1980s at the quasi-global (50°S-50°N) scale.

In addition, soil and terrain information is required. Table 2 gives an overview of the soil and terrain data used for this study. Soil data is mainly based on ISRIC SoilGrids (Hengl et al., 2017), which has a spatial resolution of 250 m but is also provided at 1000 m spatial resolution. This data is reprojected to WGS84 and spatially interpolated using nearest neighbor to the spatial resolution of 30 arc seconds applied in this study. Base saturation, gypsum, and exchangeable sodium content (ESP, sodicity) are taken from the WISE database at a spatial resolution of 30 arc seconds (Batjes, 2016). For electric conductivity, the ISRIC Global Soil Salinity Map with a resolution of 250 m is used (Ivushkin et al., 2019). In contrast to the harmonized world soil database (HWSD) (Fao et al., 2012), the ISRIC soil datasets do not contain a layer for texture class. For this reason, the texture class is determined using the sand and clay layer of SoilGrids according to the United States Department of Agriculture (USDA) triangular diagram of soil texture classes (Fao et al., 2012). For soil depths greater than 200 cm up to 50 m, the ISRIC dataset on absolute depth to bedrock (Hengl et al., 2017) is complemented with the dataset from Pelletier et al. (2016), which covers soil depths up to 200 cm.

Available soil layers can be weighted in CropSuite as required. The SoilGrids datasets provide information for six depths: 0-5 cm, 5-15 cm, 15-30 cm, 30-60 cm, 60-100 cm, and 100-200 cm (Hengl et al., 2017; Hengl et al., 2014). According to Sys et al. (1991), soil properties have different effects on crop suitability depending on the soil layer. Accordingly, we use weighting factors as proposed by Sys et al. (1991) (see Table 2). The different distribution of the soil depths between the SoilGrids data and the weighting factors by Sys et al. (1991) is taken into account by using a proportional weighting of the SoilGrids layers. Terrain data are taken from the Shuttle Radar Topography Mission (SRTM) data set (Farr et al., 2007), which are used to calculate the slope at the applied spatial resolution. Please be aware that a coarser spatial resolution generally reduces the slope, which could result in an underestimation of possible slope limitations in mountainous regions. A possible terracing could remove the restriction due to the slope but usually terraces are too small to be considered at the aggregated spatial resolution of 30 arc seconds of the SRTM data in this study.

Table 2: Soil and terrain data used in this study and the applied weighting of the different soil layers.

Parameter	Source	Weighting
Base Saturation	ISRIC Harmonized Dataset of Derived Soil Properties for the World (WISE30sec) (Batjes,	Only Top Soil

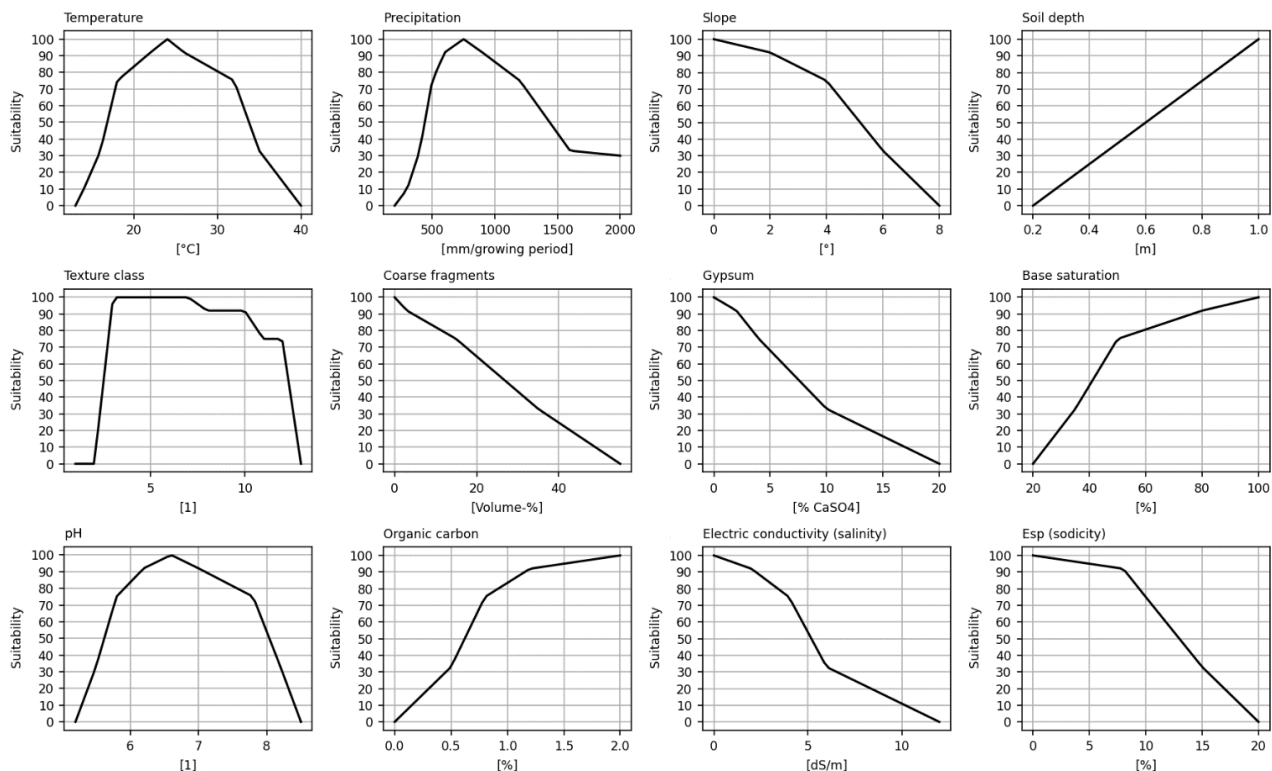
	2016)	
Coarse Fragments	ISRIC SoilGrids 250m (Hengl et al., 2017)	0 - 25 cm: 2.0 25 - 50 cm: 1.5 50 - 75 cm: 1.0 75 - 100 cm: 0.75 100 - 125 cm: 0.5 125 - 150 cm: 0.25
Electric Conductivity	ISRIC Global Soil Salinity Map (Ivushkin et al., 2019)	Only Top Soil
Gypsum Content	ISRIC Harmonized Dataset of Derived Soil Properties for the World (WISE30sec) (Batjes, 2016)	Only Top Soil
Organic Carbon Content	ISRIC SoilGrids 250m (Hengl et al., 2017)	0 - 25 cm: 2.0 25 - 50 cm: 1.5 50 - 75 cm: 1.0 75 - 100 cm: 0.75 100 - 125 cm: 0.5 125 - 150 cm: 0.25
Soil pH	ISRIC SoilGrids 250m (Hengl et al., 2017)	0 - 5 cm: 0.33 5 - 15 cm: 0.33 15 - 30 cm: 0.33
Sodicity	ISRIC Harmonized Dataset of Derived Soil Properties for the World (WISE30sec) (Batjes, 2016)	Only Top Soil
Soil Depth	ISRIC SoilGrids 2017 (Soil Depth <= 200 cm) (Hengl et al., 2017) Pelletier et al. (2016) (Soil Depth > 200 cm)	No Weighting
Texture Class	Texture class calculated from ISRIC SoilGrids 250m clay and sand content (Hengl et al., 2017) according to USDA (Fao et al., 2012)	0 - 25 cm: 2.0 25 - 50 cm: 1.5 50 - 75 cm: 1.0 75 - 100 cm: 0.75 100 - 125 cm: 0.5 125 - 150 cm: 0.25
Slope	SRTM aggregated to 30 arcsec (Farr et al., 2007)	No Weighting

108

109 Membership functions for temperature, precipitation, slope, soil depth, texture class, coarse fragments, gypsum, base
110 saturation, pH, organic carbon, electric conductivity, sodicity (Fig. 1) are defined for the considered 48 crops relying on
111 information from Sys et al. (1993), which provide membership functions for most of the considered crops. Additionally,
112 data from the EcoCrop database, which provides crop ecological requirements for more than 2500 plant species (Fao,
113 2024), is used for Cowpea, Rye, and Yams. CropSuite in principle allows the flexible addition of any further membership
114 function and dataset that is relevant for the use case.

115 Nutrient deficits, such as nitrogen content are not considered in our approach, since according to our definition of crop
116 suitability, they are not a decisive factor for the suitability of crops but rather depend on the crop management.

117 Accordingly, we do not consider any soil tillage that can affect the soil properties, such as liming, which can influence
 118 the pH value.



119
 120 **Figure 1: Membership functions exemplarily for maize** with a growing cycle of 110 days for considered climatic (mean temperature
 121 over the growing cycle, total precipitation over the growing cycle), topographic (slope), and soil constraints (soil depth, texture class,
 122 coarse fragments, gypsum, base saturation, pH, organic carbon, salinity, sodicity).

123 Sys et al. (1993) uses a classification system with 6 classes, ranging from N2 as unsuitable to S0 as highly suitable. In
 124 this study, we dismiss the N1 class due to a vague definition and differentiate three suitability classes, marginally,
 125 moderately, and highly suitable (Table 3).

126

127 **Table 3: Crop suitability classification system as used in this study compared to Sys et al. (1993).**

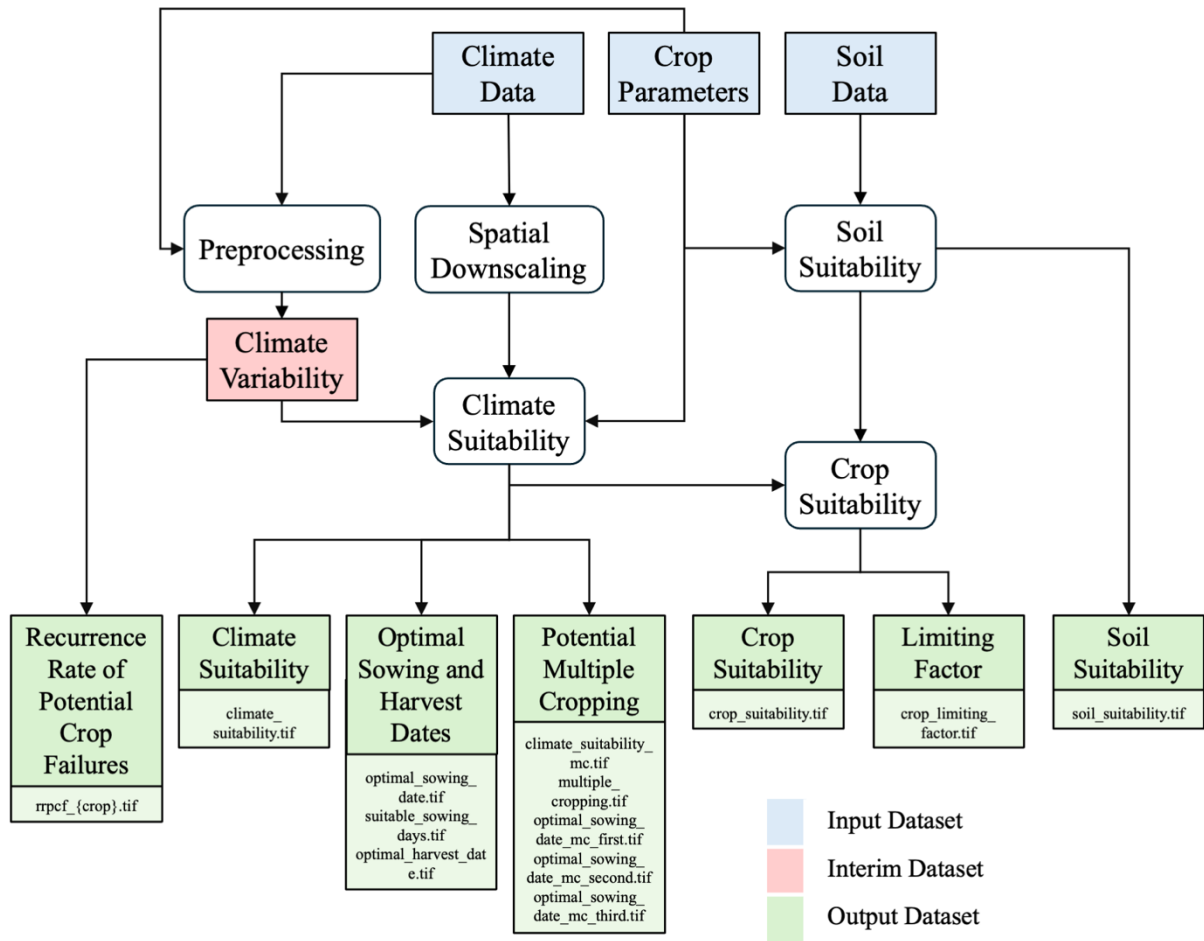
Suitability classes according to Sys et al.	Suitability range	Suitability classes used in this study
S0 (highly suitable)	100	75 – 100 (highly suitable)
S1 (very suitable)	80 – 99	
S2 (moderately suitable)	60 – 79	33 – 74 (moderately suitable)
S3 (marginally suitable)	40 – 59	1 – 32 (marginally suitable)
N1 (actually unsuitable and potentially suitable)	20 – 39	0 (unsuitable)
N2 (unsuitable)	0 - 19	

128 2.1 The CropSuite Model

129 Figure 2 shows the workflow and outputs of CropSuite, which first calculates a climate suitability (considering all climate
130 constraints) and then calculates a soil suitability (considering all soil and topography constraints). Both data records can
131 be output separately. Thereby, CropSuite applies Liebig's law of the minimum, for both the climate and the soil suitability
132 by choosing the lowest suitability value between the different soil parameters and climate variables respectively. Finally,
133 the crop suitability is calculated from the combination of both climate and soil suitability by again following Liebig's
134 law of the minimum, which means that the lowest suitability value between climate and soil suitability is chosen, since
135 it restricts overall crop suitability. The most limiting factor is identified as the parameter that imposes the greatest
136 constraint on growth for a specific crop. In addition, the magnitude of the constraint is output for each input factor.
137 Overall, CropSuite allows for a variety of outputs on optimal sowing- and harvest dates, suitable sowing days, multiple
138 cropping potentials, the limiting factor, and the recurrence rate of potential crop failures. Output data format can be set
139 to GeoTIFF or NetCDF.

140 CropSuite includes a pre-processing procedure which creates intermediate results for climate variability. Since climate
141 model data are usually available at relatively coarse spatial resolution, CropSuite has implemented a spatial downscaling
142 module for the climate data, which allows the model to be applied at very high spatial resolution from global to regional
143 to local scale. In this study, we apply a statistical downscaling to the climate data, refining the spatial resolution from 2.5
144 arc minutes to 30 arc seconds. In principle, the targeted spatial resolution can be set in CropSuite but is limited to the
145 available resolution of the additional input data, such as the soil data, whereas for the climate data, two different statistical
146 spatial downscaling methods are implemented requiring little computational effort. The first methodology is based on an
147 altitude regression for temperature (Marke et al., 2014), where the temperature gradients are extracted from the climate
148 model data itself via a moving window that can be set in size. Thereby, the extracted gradients must remain within the
149 natural boundaries for wet and dry adiabatic temperature gradients. The second downscaling methodology uses the
150 historical high-resolution spatial patterns for monthly temperature and precipitation taken from WorldClim at 30 arc
151 seconds spatial resolution (Fick and Hijmans, 2017). To downscale a coarse-resolution grid cell, all fine-resolution
152 WorldClim grid cells within the coarse-resolution cell are selected and aggregated per month. On this basis, additive
153 factors are calculated for temperature and multiplicative factors for precipitation separately for each month. Thereby the
154 sum (mean) of these additive (multiplicative) factors within the coarse-resolution cell amounts 0 (1). Considering the
155 monthly seasonality, these factors are applied to the coarse-resolution climate data, imprinting the spatial pattern of the
156 high-resolution reference data onto the coarse climate data at daily time step. Both downscaling methods conserve mass
157 and energy from the climate input data by iteratively minimizing residuals over the simulation domain. For a more
158 advanced statistical downscaling to kilometer-scale, the expert user may apply more complex topographical downscaling
159 methods (Daly et al., 1994; Fiddes et al., 2022; Karger et al., 2023) or downscaling based on machine learning (Damiani
160 et al., 2024; Wang et al., 2021) outside of CropSuite. Furthermore, we do not recommend applying the implemented

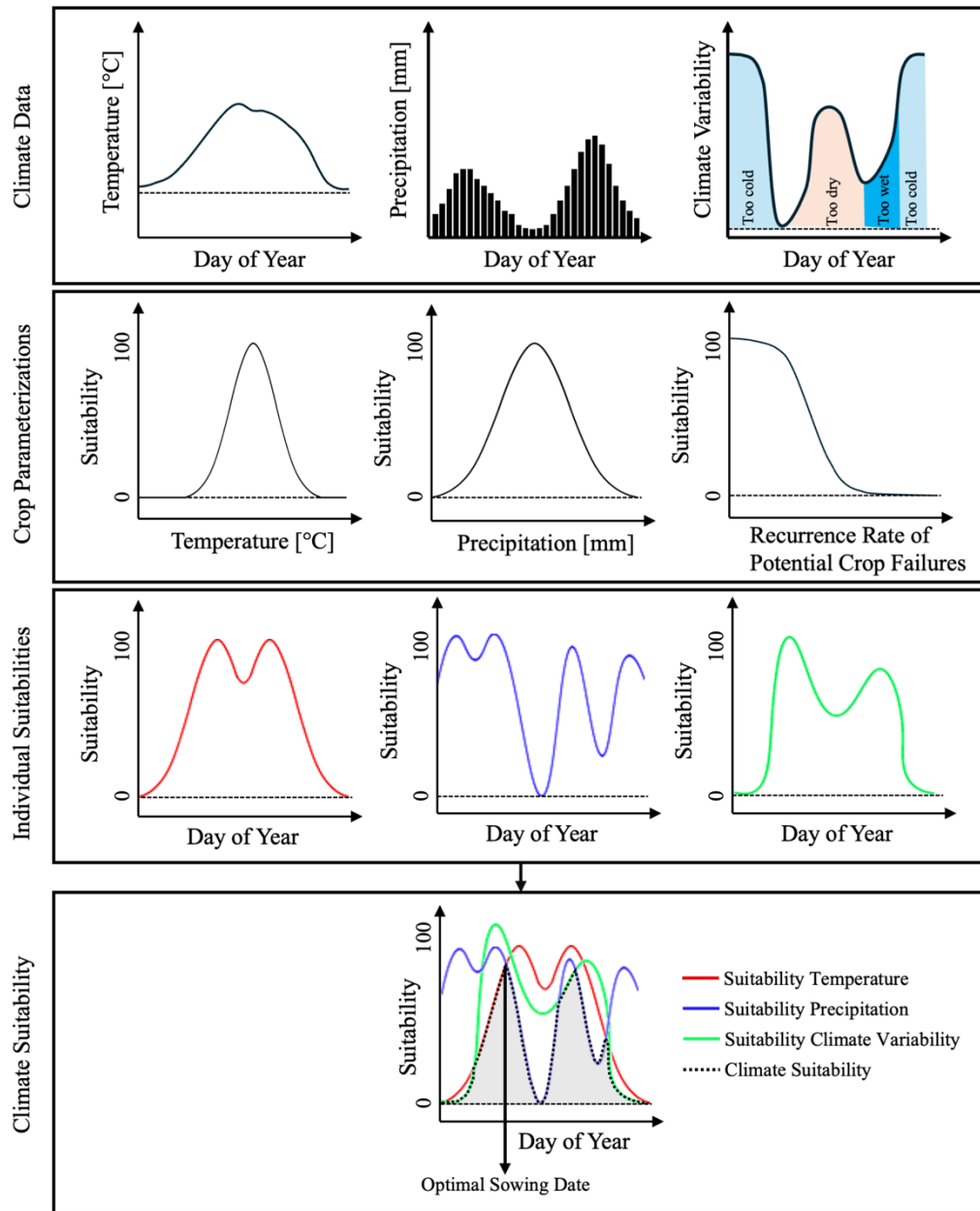
161 downscaling methods with high scaling factors from very coarse (hundreds of kilometers) to very high (single kilometer)
 162 resolution.



163
 164 **Figure 2: CropSuite workflow.** Input data in blue, intermediate results in red and output data in green. The processing steps are
 165 shown in white.

166 CropSuite requires daily climate data as an input for temperature and precipitation. As climate models tend to produce
 167 too many days with low-intensity precipitation called “drizzle bias” (Chen et al., 2021), days with aggregated daily
 168 precipitation values below 1 mm per day are considered to be dry days (Sun et al., 2006). This threshold can be set in the
 169 model. Both downscaled temperature and precipitation data and the calculated datasets for climate variability are used to
 170 calculate the climate suitability. Therefore, the crop-specific membership functions determine the suitability according
 171 to the average temperature, total precipitation and the recurrence rate of potential crop failures over the length of the
 172 growing cycle (time from sowing till maturity) for each day of year (DOY). Thereby, the suitability value for each DOY
 173 refers to the average conditions during the growing cycle from that DOY, which corresponds to the sowing date, until

174 maturity, determined by the length of the growing cycle which is set in the crop parameterization for each crop. For
175 perennial crops, the length of the growing cycle is set to 365 days. Climate suitability throughout the year is then identified
176 by selecting the minimum value (most limiting) of the three individual suitabilities for temperature, precipitation, and
177 climate variability. As shown in Fig. 3, the DOY with the highest climate suitability value over the year finally determines
178 the optimal sowing date for annual crops (optimal planting date for rice, which is not sown, but planted as a seedling in
179 wet rice cultivation). For perennial crops this is set to 1.



180

181 **Figure 3: Schematic illustration of the determination of climate suitability, the optimal sowing date and the limiting factor.** The
 182 input data shows the annual course of temperature, precipitation and the recurrence rate of potential crop failure, indicating whether it
 183 is too cold, too dry, or too wet. The crop parameterizations show the membership functions resulting in the individual suitability values
 184 for each DOY for either temperature (red line), precipitation (blue line), and climate variability (green line). Climate suitability
 185 throughout the year (black dashed line) results from the lowest of the three curves (most limiting) on any day. The highest value of
 186 climate suitability over the year finally determines the optimal sowing date. The limiting factor is the most constraining factor at this
 187 point.

188 For annual crops, CropSuite also calculates the potential for multiple harvests without considering crop rotation. Between
189 harvest and reseeding, we assume a certain time period (21 days in this study) for field work and processing, which can
190 be set flexibly in the model. Accordingly, all possible combinations of sowing dates are tested with the aim to maximize
191 climatic suitability to achieve the highest sum of climatic suitability within a year. The optimal sowing dates are selected
192 from the best sowing date combinations, resulting in one, two, or three sowing dates per year. A multiple cropping layer
193 is output that shows how often a crop can be harvested.

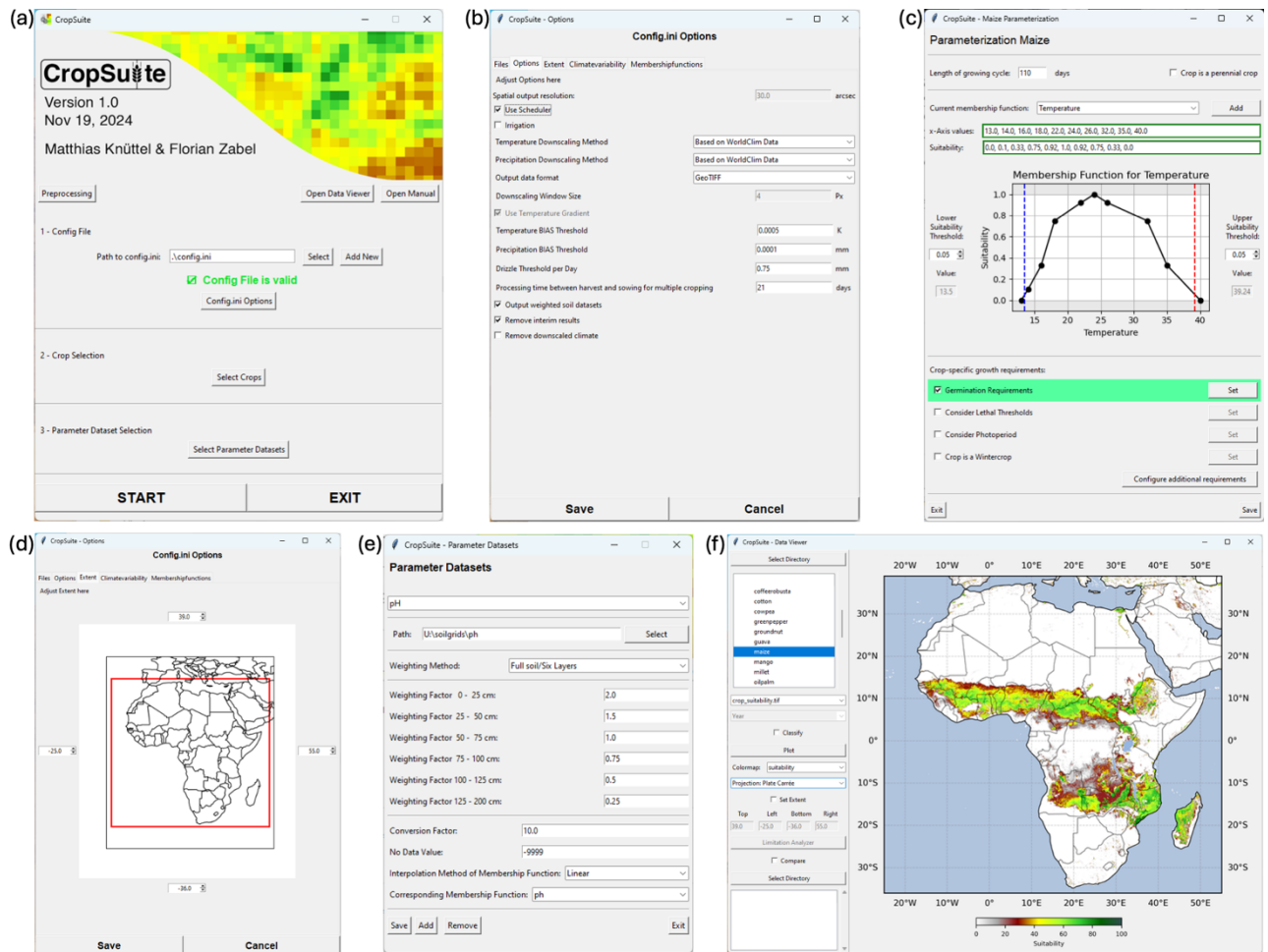
194 CropSuite distinguishes between rainfed and irrigated agricultural systems, which can be selected before starting the
195 simulation. For the irrigated case, precipitation is not considered as a constraining factor with consequences for all further
196 calculations, affecting e.g. the climate variability, the optimal sowing date, and the multiple cropping. For this study, we
197 separately simulated both, rainfed and irrigated options for all crops. In the post-processing, we combined both datasets
198 according to the irrigated areas dataset by Meier et al. (2018) (Fig. S1), which is available at 30 arc-seconds spatial
199 resolution.

200 For germination, crop-specific temperature and soil water requirements can be set in the model. The latter can be
201 considered for rainfed conditions by defining a certain amount of precipitation within a certain period of time after
202 sowing.

203 Some crops, such as soybean have a high photoperiodic sensitivity which can limit their suitability (Cober and Morrison,
204 2010; Abdulai et al., 2012). Therefore, crop-specific photoperiodic sensitivity can be considered in CropSuite by defining
205 a maximum and minimum day length in average over the growing cycle.

206 Additional lethal climatic limitations can be taken into account in CropSuite. We assume permafrost on areas with an
207 average annual temperature below 0° C, which is computed from the downscaled climate input data. A maximum lethal
208 temperature threshold of >40°C in average over the growing cycle is set for all crops (Asseng et al., 2021). In addition, a
209 minimum and maximum threshold for the lethal temperature over a certain consecutive number of days can be set in the
210 model crop-specifically. Further, the maximum number of consecutive dry days can be set dependent on the
211 crop. CropSuite allows for the consideration of vernalization requirements for winter crops. Therefore, crop-specific
212 temperature requirements with minimal and maximal temperature thresholds for a certain number of vernalization
213 effective days can be configured in the model. Accordingly, CropSuite simulates for each location, if and when these
214 vernalization requirements are fulfilled, which impacts on the length of the vernalization period and the optimal sowing
215 date. An offset of days from sowing to the start of the vernalization period can optionally be added.

216 A GUI is available for CropSuite that allows users to easily set-up the model, parameterize the crop requirements and the
217 membership functions (Fig. 4a-e), and to start the simulations. Further, new membership functions can be created, an
218 unlimited number of crop-specific requirements can be defined, and any additional data can be added, which can be
219 flexibly assigned to the defined membership functions (Fig. 4e). Moreover, new crops or crop varieties can be added.
220 The GUI also allows for the visualization, analysis and comparison of the results (Fig. 4f).



221

222

Figure 4: Graphical User Interface of CropSuite. (a) shows the main screen, (b) exemplarily shows available model settings, (c) shows the available options for crop parameterizations exemplarily for maize, (d) shows the window to set-up the simulation domain, (e) exemplarily shows the set-up of a parameter dataset for soil pH, and (f) shows the integrated data viewer in CropSuite.

223

224

225

2.2 Climate Variability

226

227

228

229

230

231

232

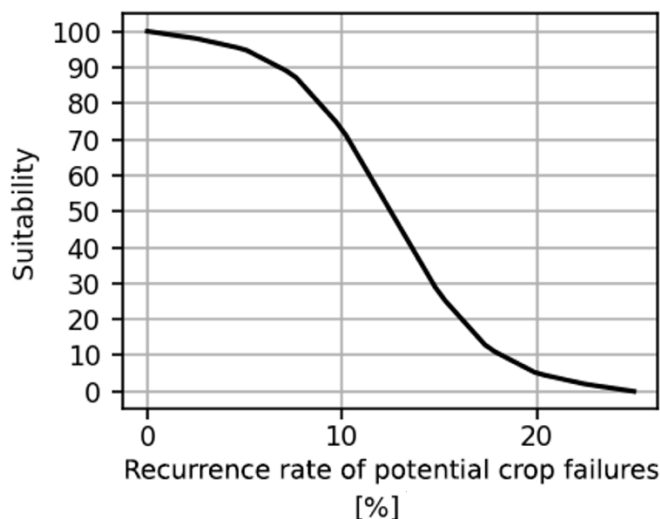
233

In addition to several improvements and redesigns, one of the most important advancements in CropSuite is the consideration of climate variability for the assessment of crop suitability. Usually, crop suitability models consider long-term climate averages, e.g. 10, 20 or 30-year periods and climatic trends that affect crop suitability (Ramirez-Villegas et al., 2013; Schneider et al., 2022b). They are not designed so simulate seasonal yields, as for instants mechanistic crop models do (Jägermeyr et al., 2021). However, existing crop suitability approaches may overestimate crop suitability when only long-term averages are considered, because a high climatic variability may result in a high frequency of unsuitable years, which would result in crop failures. This would however significantly increase the risk for farmers that require stable and plannable conditions. As a result, a farmer may conclude that the risk of crop failures due to unstable climate

234 conditions in a certain region is too high for being suitable for crop cultivation. As such, climate variability is not a purely
235 ecological limitation but depends on the socio-economic circumstances of how farmers deal with the risk of crop failure.
236 We developed an approach that allows for the consideration of climate variability, and thus the implicit integration of
237 socio-economic limitations in the suitability assessment of crops.
238 Therefore, we specify a crop-specific lower and upper threshold for temperature and precipitation. We recommend these
239 thresholds between the higher and lower 5% and 10% suitability values of the crop-specific membership function,
240 respectively (Figs. 1, 4c). If the suitability of the membership function does not approach 0 at its high (low) limit, we
241 recommend setting the threshold to the highest (lowest) value of the membership function. This is the case for the wet
242 limit of the precipitation membership function for maize (see Fig. 4c). For each year within a given period of time (here
243 we use 20-year time periods), it is tested and totaled, how often these thresholds exceed or fall below during the growing
244 cycle for all possible sowing dates (January 1st until December 31st). As a result, a variability dataset is generated for each
245 DOY, indicating the number of years in which at least either the temperature or the precipitation exceeds or falls below
246 the threshold values. The number of years is divided by the length of the time period (here 20 years) to obtain the
247 recurrence rate of potential crop failures. This data can be stored as a two-dimensional raster file for perennial crops or
248 as a three-dimensional raster file for non-perennial crops, with each of the 365 DOYs representing the condition for the
249 respective sowing day.

250 For rainfed agricultural systems, cases that are considered for climate variability include excessively high or low
251 temperatures and precipitation, while for irrigated agricultural systems, only excessively high or low temperatures and
252 excessively high precipitation are considered, to address potential water logging, plant diseases or root rotting. Due to
253 computational limitations, the preprocessing of the climate variability is carried out at the resolution of the input climate
254 data (2.5 arc minutes) and is further interpolated bilinearly to the output resolution of 30 arc seconds.

255 Finally, we introduce a membership function defining the impact of climate variability on crop suitability. As shown in
256 Fig. 5, a sigmoid is adopted for the course of the function. According to expert knowledge, we set this sigmoid function
257 in a way that it reduces suitability to 0 when the recurrence rate of potential crop failure is greater than once every 4 years
258 (25%). However, this function may be different in different parts of the world and different between crops (see
259 Discussion).



260

261

262

Figure 5: Membership function for climate variability showing the impact of the recurrence rate of potential crop failures on crop suitability. The seasonal recurrence rate is shown in percent.

263

3 Model evaluation

264

Crop suitability is difficult to validate or measure, nor is it equivalent to agricultural yields or production values. However, a comparison with other studies and data can provide valuable information and build confidence in the approach.

265

266

3.1 Comparison with Harvested Area

267

In principle, a crop should be suitable where it is already cultivated. According to this premise, we compare the suitable area simulated with CropSuite with the harvested areas from the global spatially-disaggregated crop production statistics data for 2020 (MapSPAM 2020 v1.0) produced by the International Food Policy Research Institute (IFPRI) using the Spatial Production Allocation Model (SPAM) (Ifpri, 2024). The CropSuite results for Africa consider climate variability and are combined for irrigated and rainfed areas according to Meier et al. (2018). While MapSPAM relates to the year 2020, our simulations refer to the 1991-2010 time period, which could be a source of uncertainty. Nevertheless, we used MapSPAM 2020 instead of other available versions of MapSPAM, since it includes 32 crops from our investigation and is the latest released version of MapSPAM. A comparison between CropSuite and different MapSPAM versions is shown exemplarily for maize in Fig. S2, revealing a considerably better fit with CropSuite in the MapSPAM 2020 version. For comparison, harvested areas below 10 ha per pixel are excluded from the calculation and the high spatial resolution of the CropSuite model output is resampled to the same spatial resolution (5 arc minutes) than the MapSPAM 2020 data. Figure 6 depicts the results of this analysis for all crops, where green and purple bars represent areas that are suitable, while orange and green areas represent harvested areas in MapSPAM. Purple bars indicate suitable areas that are currently not used by the respective crop. While green areas are also identified as being suitable in our approach, orange areas are

268

269

270

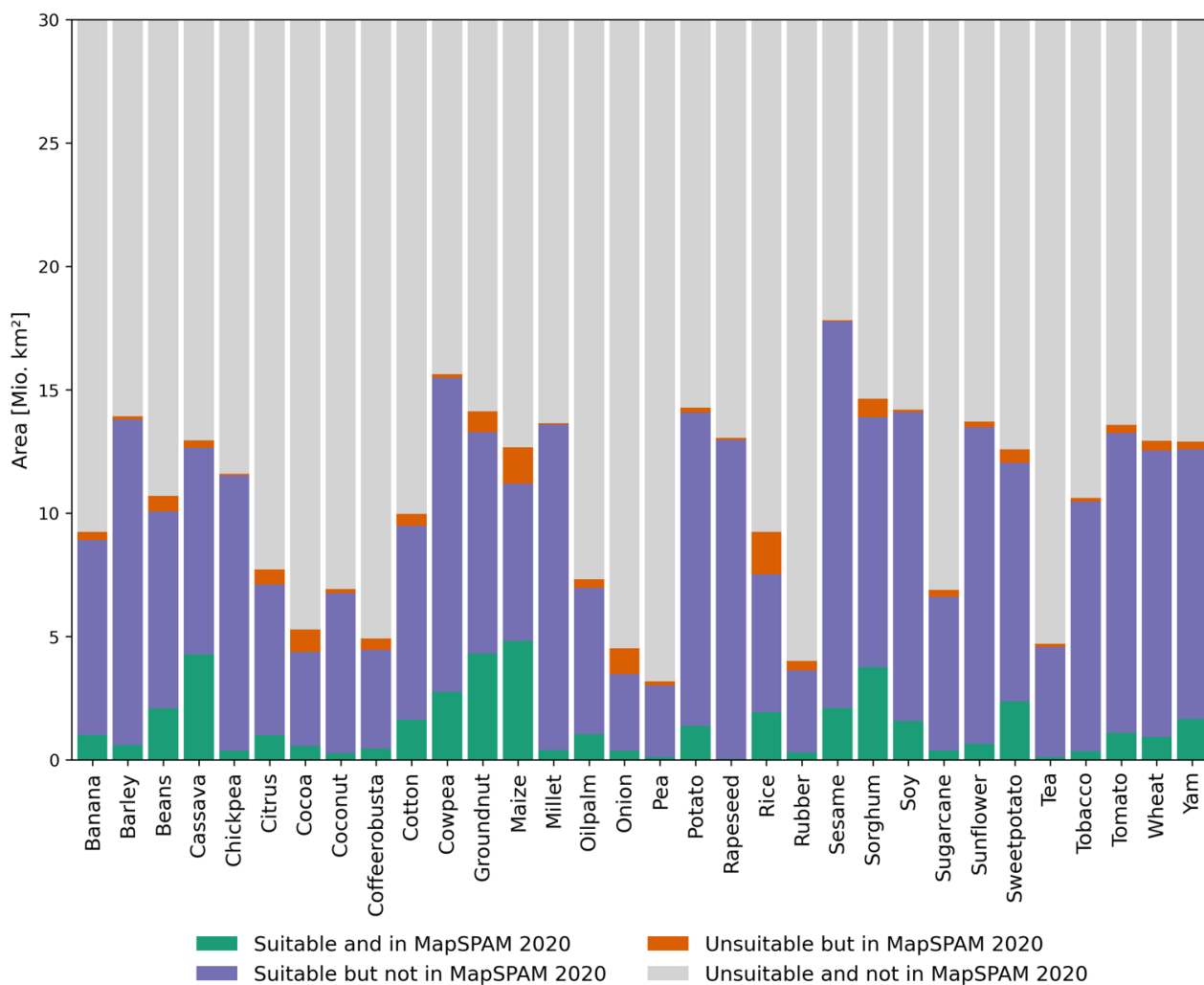
271

272

273

274

281 not suitable in CropSuite despite the respective crop is harvested according to MapSPAM. Crops with the largest
 282 mismatching areas are rice, maize, and onion (Fig. 6). Most crops show a small proportion of orange to green areas,
 283 except for onions, rapeseed, cocoa, pea, rubber, tea, coffee, and rice (Fig. S3). This can have various causes, such as data
 284 uncertainty of climate, soil and irrigation data (Avellan et al., 2012), incorrect membership functions, the use of different
 285 crop varieties, or an incorrect localization of the cultivation areas in MapSPAM due to high uncertainties in the underlying
 286 national statistical data, especially in African countries (Yu et al., 2020), or applied crop management practices that could
 287 level out ecological limitations.

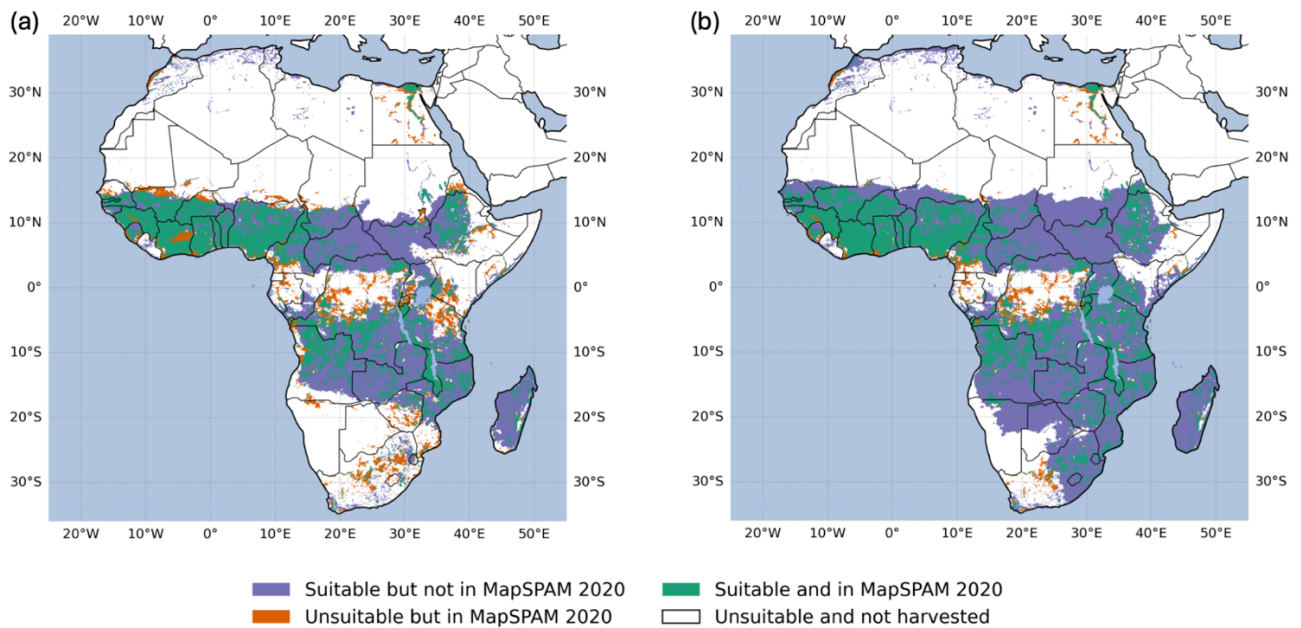


288

289 **Figure 6: Comparison of CropSuite with MapSPAM 2020 for all matching crops.** CropSuite results combine irrigated and rainfed
 290 areas according to Meier et al. (2018) and consider climate variability. Areas on which the respective crop is harvested according to
 291 MapSPAM and which are suitable according to CropSuite are shown in green, areas that are suitable but on which the crop is not
 292 harvested are shown in purple. Areas that are unsuitable but are harvested according to MapSPAM are shown in orange, while
 293 unsuitable areas that are not harvested according to MapSPAM are shown in grey.

294 Figure 7a shows the spatial comparison between crop suitability and harvested areas for maize. Areas where maize is
 295 harvested according to MapSPAM, although CropSuite has identified these areas as unsuitable, are found mainly in
 296 Egypt, the northern Sahel, the Congo Basin, as well as parts of Cameroon, Gabon, Kenya, Tanzania, Zimbabwe and
 297 South Africa. Figure 7b shows the comparison ignoring the impact of climate variability on crop suitability. Disregarding
 298 climate variability results in large (blue) areas, which are considered suitable but are no harvest areas according to
 299 MapSPAM, especially along the dry belts (15°N and 20°S). Our approach considering climate variability (Fig. 7a)
 300 reduces these blue areas, but induces some mismatches, where MapSPAM indicates harvested areas and CropSuite shows
 301 no suitability (red areas). We find that the mismatching areas along the dry belts (including the Sahel) and in eastern
 302 Africa (Tanzania, Kenya) are often associated with limits due to climate variability. This indicates that the thresholds for
 303 climate variability (section 2.2) and the membership function (Fig. 5) might be parameterized slightly too exclusive.
 304 However, some of these regions might be used as cropland by smallholders or subsistence farmers despite the high risk
 305 of crop failures.

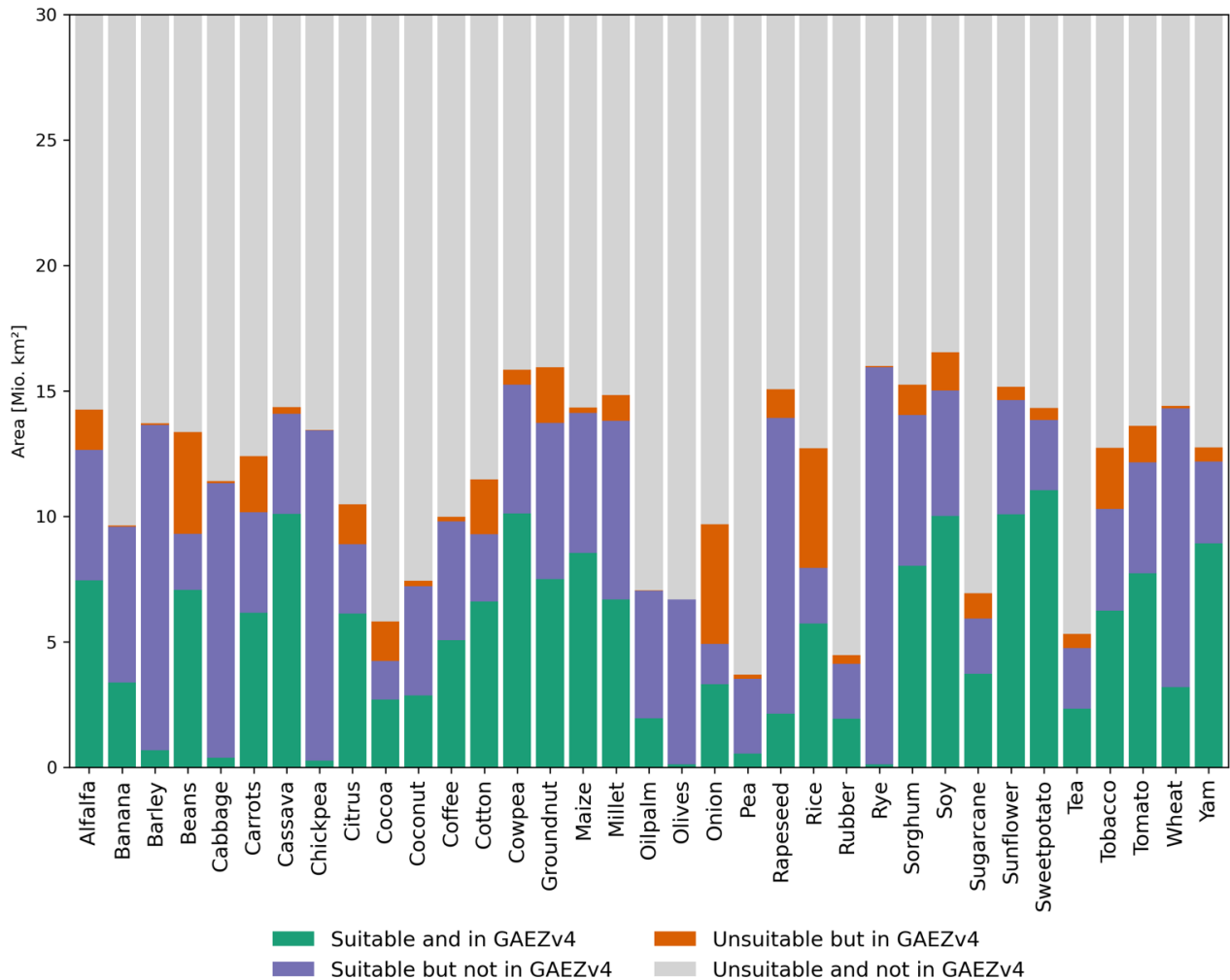
306 While in the inner tropics, the reason for limited crop suitability can primarily be attributed to soil acidity (pH), indicating
 307 possible uncertainties with used SoilGrids dataset, differences in Egypt mainly result from discrepancies according to
 308 different assumptions on irrigated areas.



309 **Figure 7: Comparison of CropSuite with MapSPAM 2020 for maize.** (a) shows the comparison with consideration of climate
 310 variability in CropSuite, while climate variability is not considered in (b). Areas on which the respective crop is harvested according
 311 to MapSPAM and which are suitable according to CropSuite are shown in green, areas that are suitable but on which the crop is not
 312 harvested are shown in blue. Areas that are not suitable but are harvested according to MapSPAM are shown in red. Unsuitable areas
 313 that are not harvested according to MapSPAM are shown in white.
 314

315 3.2 Comparison with GAEZ

316 A state-of-the-art climate-edaphic suitability assessment for crops is provided by the Global Agro-Ecological Zones
317 (GAEZ) v4 (Fischer et al., 2021). For comparison with CropSuite, we used GAEZ data for the time period 1981-2010
318 for high input level, rainfed conditions and the option ‘all land in grid cell’. The high input level refers to advanced
319 management assumptions (fully mechanized, optimum application of nutrients and chemical pest, disease and weed
320 control) (Fischer et al., 2021), which correspond best to the assumptions made in CropSuite for this study. The suitability
321 range of the GAEZ data is transformed to the classification system as shown in Table 3. The CropSuite data for rainfed
322 conditions is resampled (using the average) to the same spatial resolution of 5 arc minutes than the GAEZ data. For this
323 comparison, we use CropSuite data without climate variability, since the GAEZ approach does not consider climate
324 variability as well. Coffee was compared against the best type of robusta and arabica, as done in the GAEZ data (Fischer
325 et al., 2021). Overall, there are large overlaps between the GAEZ and CropSuite (Fig. 8). Generally, CropSuite identifies
326 larger suitable areas than GAEZ for Africa (purple bar in Fig. 8), particularly for barley, cabbage, chickpea, rapeseed,
327 rye and wheat. A main reason for differences may be due to different underlying soil data, GAEZ uses the HWSD while
328 CropSuite uses the SoilGrids data. As an example, we found abrupt changes in the GAEZ results, especially between
329 borders (e.g. between Angola and Zambia), which follows patterns of the underlying HWSD, which is a known issue
330 (Dewitte et al., 2013). The consideration of climate variability in CropSuite mainly results in larger areas that are
331 unsuitable in CropSuite but still suitable in GAEZv4 (orange bars) (Fig. S4).



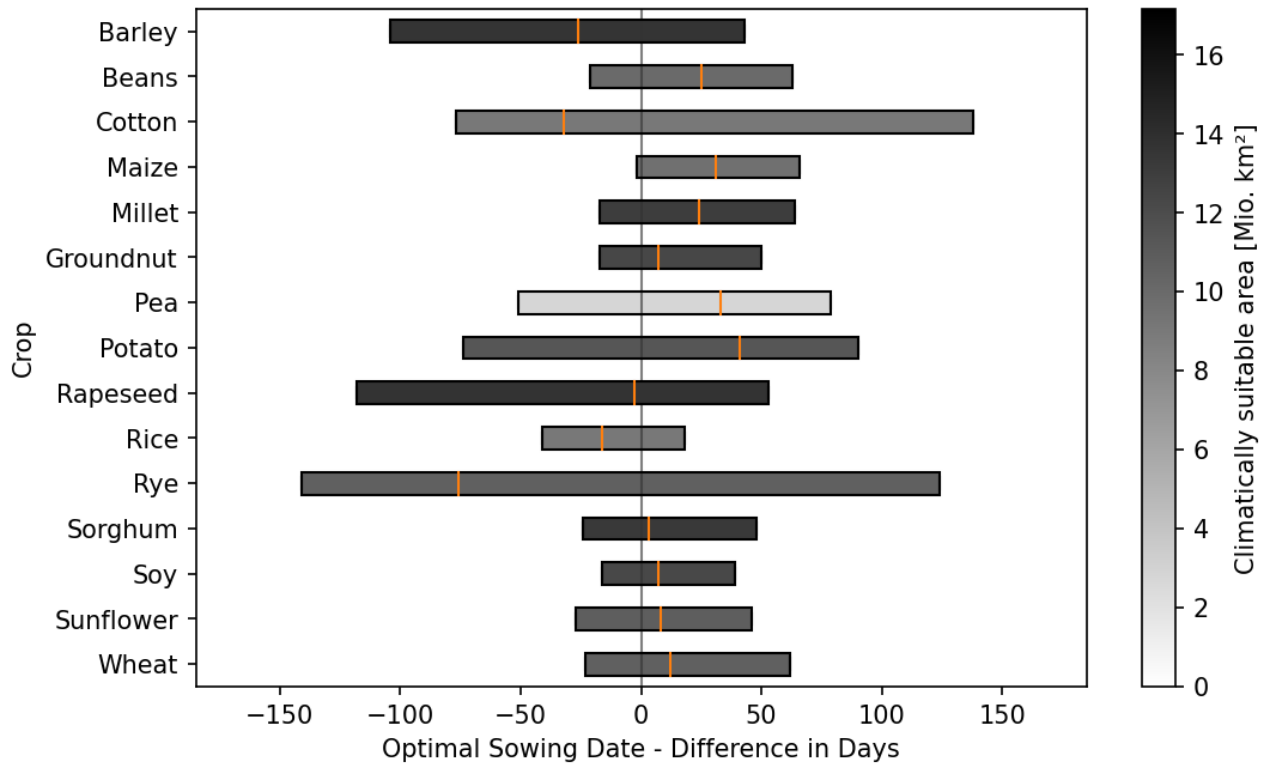
332

333 **Figure 8: Comparison between CropSuite and GAEZv4 suitability data for all matching crops.** CropSuite results are shown
 334 without consideration of climate variability. Areas that are suitable in both data, CropSuite and GAEZv4 are shown in green, areas
 335 suitable in CropSuite but not suitable in GAEZv4 are shown in purple. Unsuitable area in CropSuite that is suitable in GAEZv4
 336 is shown in orange. Areas that are unsuitable in both data are shown in grey.

337 **3.3 Comparison of Optimal Sowing Dates with the GGCM Crop Calendar**

338 Another method of validation involves comparing the optimal sowing dates computed with CropSuite with the crop
 339 calendar from the Global Gridded Crop Model Intercomparison (GGCM), which is available globally for a variety of
 340 different crops at half degree spatial resolution (Jägermeyr et al., 2021). Figure 9 illustrates the average differences of the
 341 sowing dates across Africa, averaged for the matching crops between the two datasets. The comparison is performed at
 342 a spatial resolution of 30 arc seconds (Fig. 9) and at half degree resolution (see Fig. S5). For the high spatial resolution,
 343 the GGCM data are interpolated to 30 arc seconds using nearest neighbor. Unlike CropSuite, which displays the optimal

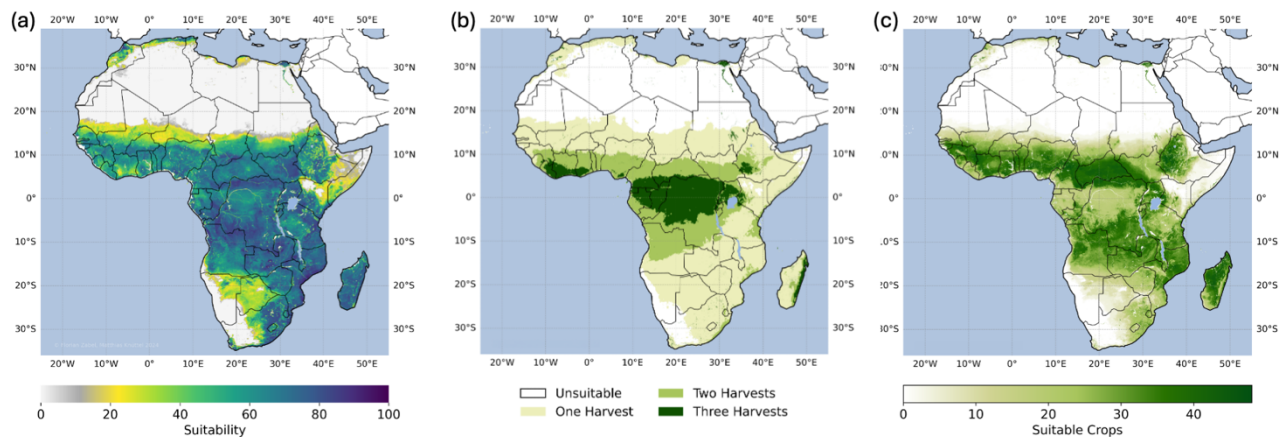
344 sowing date, the GGCM data show the actual sowing date based on extrapolated statistics. Thus, there might be
 345 differences between the optimal and actual sowing dates. It must also be considered that the GGCM crop calendar is
 346 based on statistics that apply to discrete areas at relatively coarse half degree spatial resolution, while CropSuite was
 347 simulated at a pixel accuracy of 30 arc seconds spatial resolution. In fact, the median differences are mostly within one
 348 month of the GGCM crop calendar, which generally indicates a high agreement. Generally, we found that a greater
 349 distance to the equator potentially increased the discrepancy between the two data. As an example, in tropical climates
 350 with occurring dry and rainy seasons, a shift from one rainy season to another rainy season might result in a greater
 351 discrepancy. Also, we found that the distribution of sowing dates over the year was less concentrated in CropSuite, which
 352 could be a result of the higher spatial resolution (see Fig. S6). At the coarse resolution, the difference between the two
 353 datasets is less and the spread is smaller (Fig. S5).



354
 355 **Figure 9: Comparison of the optimal sowing dates of CropSuite with the actual sowing dates of the GGCM crop calendars.**
 356 The area-weighted shift of the sowing date in days is shown for all matching crops. Negative values mean an earlier sowing date in
 357 CropSuite, positive values mean a later sowing date in CropSuite compared to the GGCM Crop Calendar. The bars show the 5th and
 358 95th percentile, the orange marker shows the median. The color of the bars indicates the climatically suitable area for the whole of
 359 Africa. Irrigated areas are considered according to Meier et al. (2018). The comparison is performed at 30 arc seconds spatial resolution
 360 for both datasets.

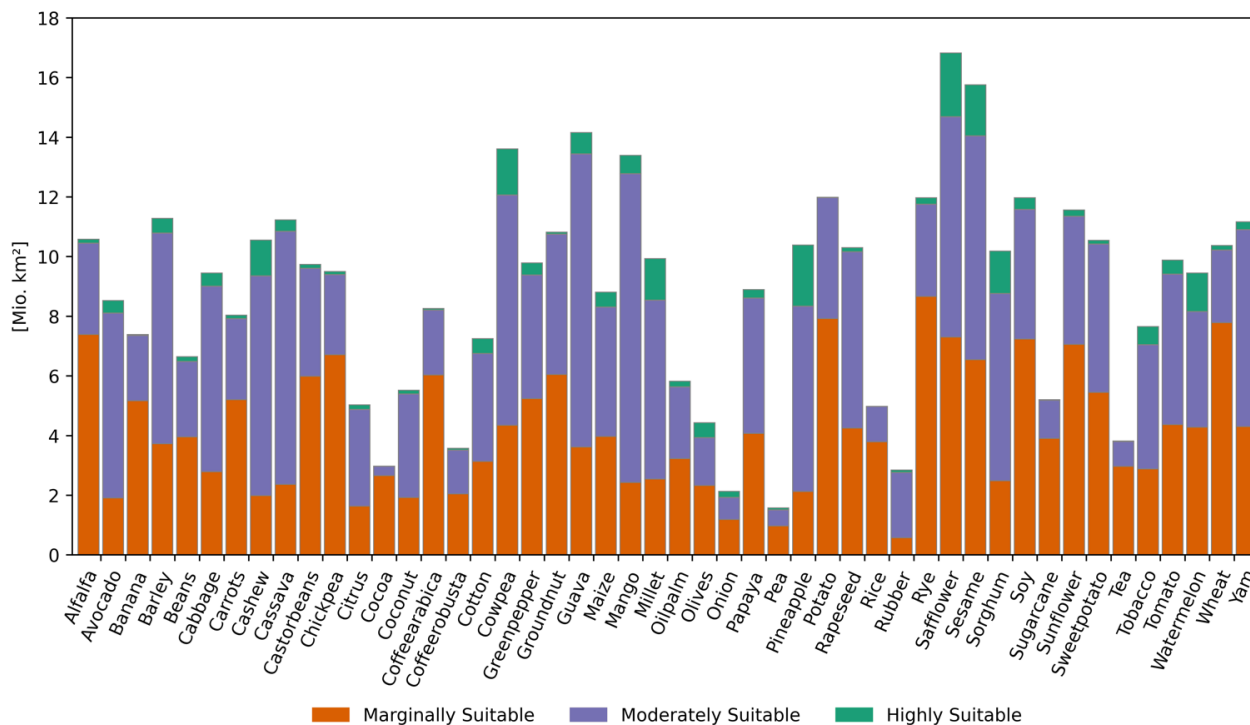
361 4 Simulation Results

362 Crop suitability is simulated for historical climate conditions (1991-2010) for rainfed and irrigated conditions. Figure 10a
363 illustrates the overall crop suitability, showing for each location the value for the most suitable of all considered crops.
364 Irrigation is considered according to the currently irrigated areas for Africa (Meier et al., 2018), such as along the Nile
365 river in Egypt (see Fig. S1 for irrigated areas in Africa). In total for Africa, 5.7 million km² are highly suitable, 10.6
366 million km² are moderately suitable, 3.3 million km² are marginally suitable and 10.4 million km² are not suitable for
367 crop cultivation. Mainly between 10° N and 10° S, a high potential for multiple cropping exists with the possibility of
368 two or three harvests per year (Fig. 10b). Looking at the number of crops suitable for cultivation (Fig. 10c), a large
369 proportion of the considered crops can grow particularly along the wet savannahs, which gives these regions plenty of
370 opportunities for cultivation. In contrast, only a few crops are suitable for the inner tropics and the dry savannahs, which
371 limits the possibilities for switching between crops.



372
373 **Figure 10: (a) Overall crop suitability, (b) potential multiple cropping, and (c) number of suitable crops under historical climate**
374 **conditions from 1991 to 2010.** Irrigated areas are considered according to Meier et al. (2018). The overall crop suitability (a) and the
375 potential multiple cropping (b) are each shown for the most suitable crop at each location. The maximal number of suitable crops
376 results from the number of 48 considered crops (see Table 1). Figure 10a is shown with different colormap in the supplement (Fig.
377 S7).

378 Figure 11 shows the suitable area for each of the simulated crops for Africa. The five crops with the largest suitable areas
379 in Africa are safflower (16.82 mio km²), sesame (15.76), guava (14.15), cowpea (13.61), and mango (13.39).



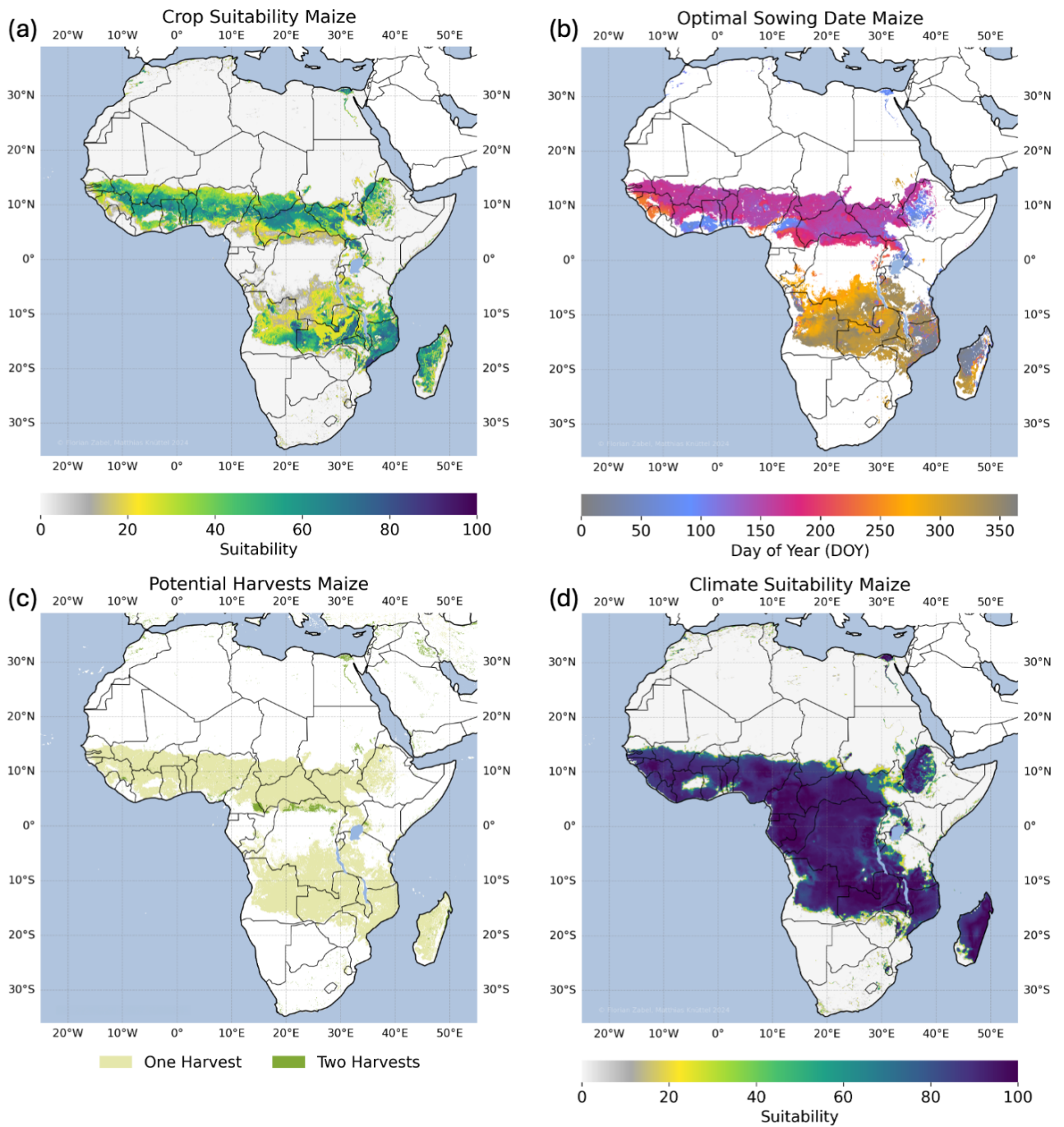
380

381 **Figure 11: Marginally, moderately and highly suitable areas for all 48 crops under historical climate conditions from 1991 to**
 382 **2010 for Africa.** Suitability classes are chosen according to Table 3. Irrigated areas are considered according to Meier et al. (2018).

383 Figure 12a exemplarily shows the crop suitability simulated for maize. The maps for all crops are provided via Zenodo
 384 (see Data Availability). Maize is highly suitable along a strip of the 10° N and the 20° S parallel as well as large parts of
 385 Mozambique and Madagascar. In total, 0.49 million km² are highly suitable, 4.34 million km² are moderately suitable,
 386 3.97 million km² are marginally suitable and 21.23 million km² are unsuitable.

387 The optimal sowing date for single cropping (Fig. 12b) for maize shifts with latitude from the northern hemisphere across
 388 the equator to the southern hemisphere. Figure 12c shows the potential number of potential harvests per year for maize.
 389 Climate conditions allow up to two harvests per year in some parts of Congo and Cameroon and in the irrigated areas e.g.
 390 along the Nile river. Optimal sowing dates for first and second sowing on areas suitable for multiple cropping are shown
 391 in Fig. S8.

392 Figure 12d shows the climate suitability for maize, which just considers climatic constraints for the suitability of maize.
 393 In comparison to the crop suitability map (Fig. 12a), more areas are suitable and suitability is substantially higher, if soil
 394 and topography are not considered and therefore do not limit or reduce crop suitability.

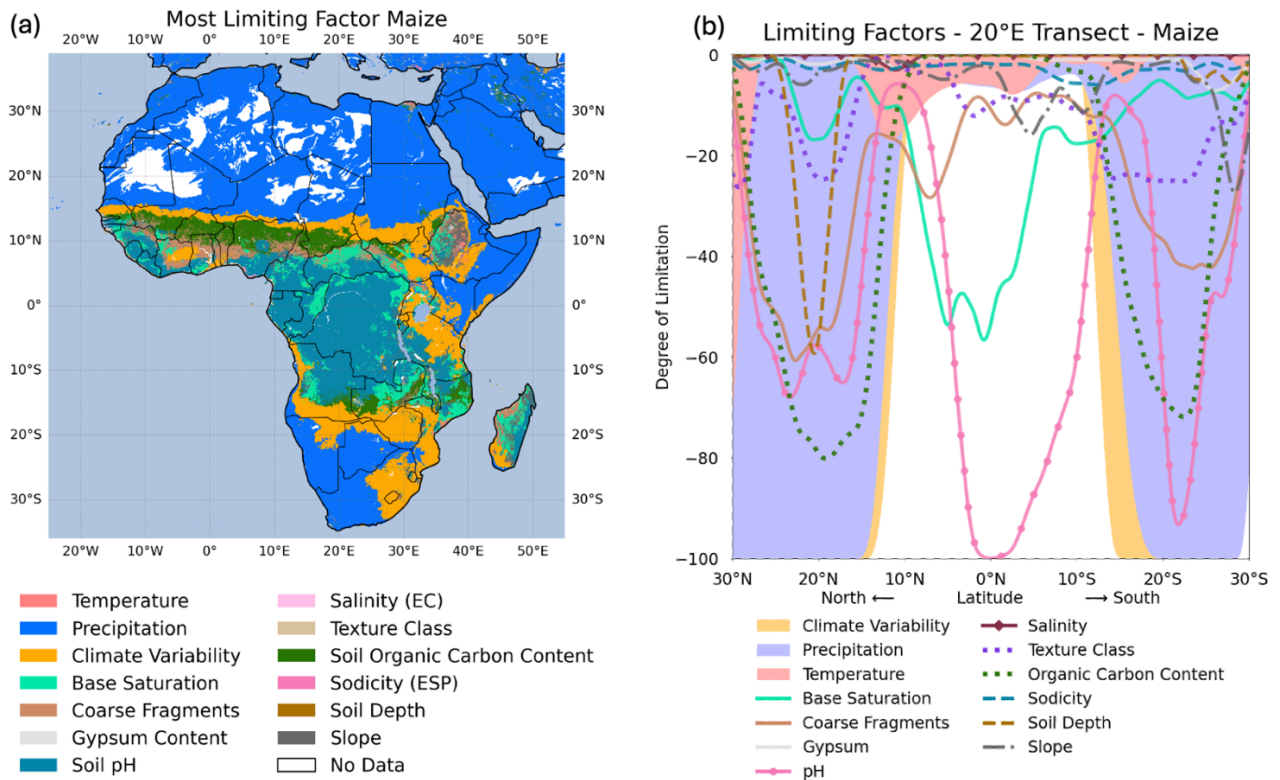


395

396 **Figure 12: (a) Crop suitability, (b) optimal sowing date for single cropping, (c) potential multiple cropping, and (d) climate**
 397 **suitability for maize under historical climate conditions from 1991 to 2010. Irrigated areas are considered according to Meier et**
 398 **al. (2018). Figure 12a is shown with different colormap in the supplement (Fig. S9).**

399 The most limiting factor is shown in Fig. 13a. While low precipitation prevents maize from being suitable in large parts
 400 of Africa in the arid deserts, soil is predominantly restricting suitability in tropical regions. Particularly pH is the most
 401 limiting factor in the humid tropics, such as the Congo Basin, where soils are too acid for growing maize. A large band
 402 along the drylands highlights regions where inter-annual climate variability is most limiting maize suitability (in orange,
 403 Fig. 13a). Here, climate conditions are unstable for maize cultivation, and the recurrence rate of potential crop failures is
 404 larger than 25% (every fourth year). For maize, climate variability is limiting crop suitability on 4.4 million km² for
 405 Africa (Fig 13a).

406 Figure 13b shows the degree of limitation for all considered climate, soil and terrain factors along a transect following
 407 the 20° E from North to South. In the Sahara, several factors, including temperature, organic carbon content, and soil pH,
 408 are not in an optimal range, while precipitation and the climate variability are the most limiting (note that climate
 409 variability is by definition a limiting factor if precipitation and/or temperature are limiting factors). Due to the unfavorable
 410 soil conditions, irrigation would only slightly improve maize suitability here. Between 15° N and 5° N, the limitations of
 411 all factors are relatively low. Here, coarse fragments and base saturation are most limiting. The tropical areas along the
 412 transect between 5° N and 10° S are mainly constrained by soil pH. Accordingly, soil management or practices that
 413 increase pH in these regions would have a significantly positive impact on crop suitability in this region, since no other
 414 factor has such a strong impact on maize suitability. Further south, low precipitation again mostly limits maize suitability.



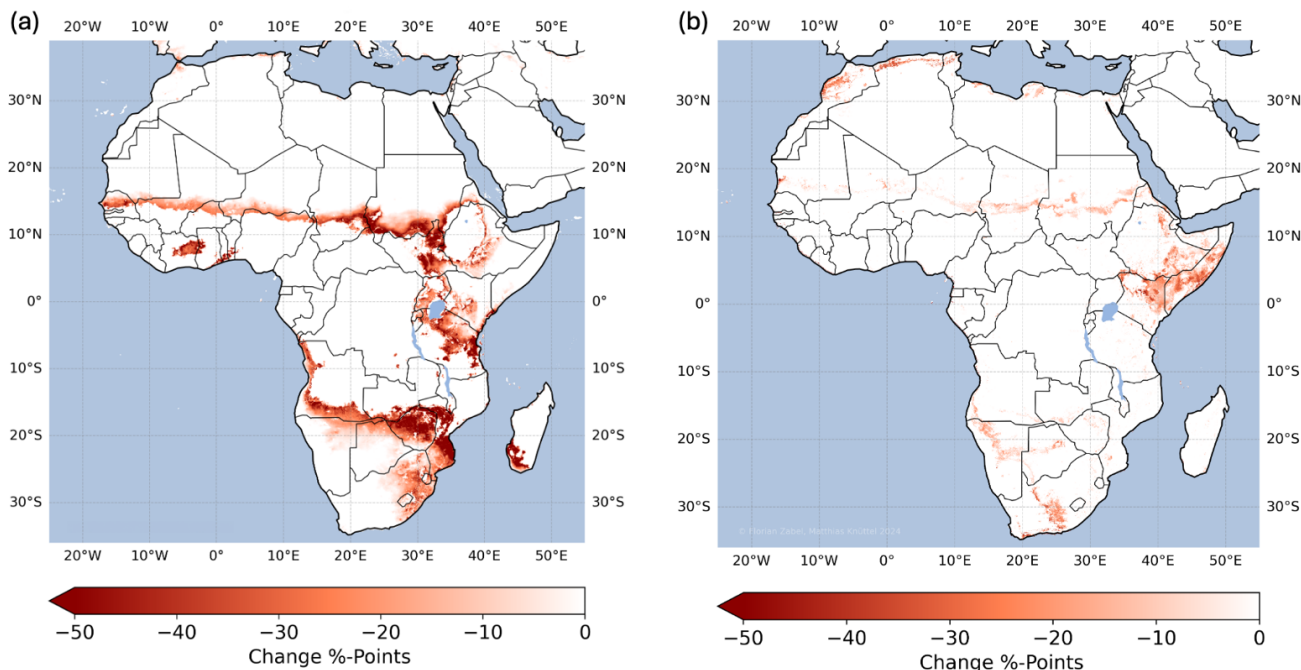
415

416 **Figure 13: Limiting factors.** (a) Most limiting factor of the crop suitability for maize under historical climate conditions from 1991
417 to 2010. (b) shows the degree of limitation of all factors along a transect of the 20° East from 30° North to 30° South. The most limiting
418 factors are displayed with priority according to the order in the legend in (a), if more than one factor fully limits the suitability. For
419 visualization, the shapes in (b) are smoothed using a moving average. Irrigated areas are considered according to Meier et al. (2018)
420 in (a) and are not considered in (b).

421 The consideration of climate variability significantly reduces climate suitability for maize as shown in Fig. 14a, mainly
422 in the transition area between dry savannah and desert in the Sahel zone, in Burundi and Tanzania in Eastern Africa, and
423 in the southern part of Africa in Angola, Zambia, Zimbabwe, Mozambique, South Africa, and the southern part of
424 Madagascar. In total, climate variability reduces climate suitability on more than 5.4 million km².

425 Optimal sowing dates also shift when considering climate variability, since the algorithm identifies the best suitable time
426 window for the growing cycle over the year (Fig. S10). As a result, optimal sowing for maize considerably shifts in
427 Tanzania, Mozambique and Madagascar.

428 Over all crops, Fig. 14b shows the impact of climate variability on the overall crop suitability. In this case, overall crop
429 suitability is reduced on 2.2 million km², mainly reduced in Somalia, Kenya, Ethiopia, South Africa, and the Maghreb
430 countries of Morocco, Algeria, Tunisia, and Libya. These regions generally show a high vulnerability to climatic
431 variability. Climate variability also reduces the potential for multiple cropping in general over all crops on more than 2.3
432 million km² (Fig. S11).



433 **Figure 14: Impact of the consideration of climate variability on crop suitability (a) for maize (b) for the overall crop suitability**
434 **of all crops under historical climate conditions from 1991 to 2010.** Irrigated areas are considered according to Meier et al. (2018).
435

436 5 Discussion

437 We found that the consideration of climate variability significantly affects crop suitability, multiple cropping, and optimal
438 sowing dates in Africa. Our approach allows to adjust the risk aversion of farmers by adjusting the thresholds for climate
439 variability (section 2.2.) and the membership function (Fig. 5). The shape of this function may differ between crops and
440 regions and might be influenced by several socio-economic factors, such as the degree of mechanization, financial
441 possibilities, and the availability of crop insurances, which is likely to reduce risk aversion of farmers. We suggest the
442 function as shown in Fig. 5 as a broad and general solution which is primarily designed to represent risk aversion of
443 commercial farms. In our comparison analysis for maize (section 3), reference data showed some cultivation in the
444 regions we identified as unsuitable due to the high recurrence rate of potential crop failures caused by high climate
445 variability (Fig. 7). In some regions, despite the high risk of crop failures, land might be cultivated by smallholders or
446 subsistence farmers that have no other choice but to cultivate these lands. However, we admit that the tuning of the
447 climate variability thresholds and the membership function requires more research, and the optimal results will vary
448 depending on crop and region. CropSuite offers the platform and the possibilities to conduct such assessments.

449 The results of CropSuite (section 4) are subject to uncertainties in the applied climate, soil, terrain, and irrigation data as
450 well as the membership functions (Fig. 1). Soil and terrain data are assumed to be static, although management could
451 influence soil properties such as pH, and terracing could reduce slope limitations. The applied climate data from CHIRPS
452 and CHIRTS are found to be particularly valuable in regions, where climate stations are sparse. Over Africa, CHIRPS is
453 successfully validated (Dinku et al., 2018) showing good performance (Lemma et al., 2019; Muthoni et al., 2019). Verdin
454 et al. (2020) also report good agreement of CHIRTS over Africa, however with a poor performance over central Africa,
455 the Horn of Africa, and parts of northern Mali. Generally, both data sets rely on station data to correct the satellite
456 estimations, which is why uncertainties for very data-scarce regions remain. To apply CropSuite in regions outside 50°S-
457 50°N, or to larger time periods before the 1980s, the user of CropSuite could also rely on global high-resolution climate
458 reanalysis, such as ERA5 (Hersbach et al., 2020). For the African continent, ERA5 reanalysis shows large improvements
459 over its predecessor ERA-Interim (Gleixner et al., 2020). Still, considerable deviations in precipitation from CHIRPS are
460 reported, e.g., wet biases over Uganda (Gleixner et al., 2020) and a dry bias over the western Sahel (Gbode et al., 2023),
461 where CHIRPS is applied as reference. We therefore assume that CHIRPS and CHIRTS are very suitable climatic data
462 sets to investigate our example of maize suitability in Africa. The soil profiles used for the generation of the SoilGrids
463 show a heterogeneous distribution, with large gaps over central Africa, which is why Hengl et al. (2017) attribute
464 uncertainty in the data to the under-sampling. They argue that a few hundred additional profiles in under-sampled areas
465 could massively improve the resulting SoilGrids.

466 The membership functions derived by Sys et al. (1993) are widely applied but are also governed by inherent uncertainties.
467 Herzberg et al. (2019) argue that the assessment by Sys et al. (1993) is not detailed enough to capture specific features of
468 small areas. They find that Sys et al. (1993) would consider a hilly area in tropical Vietnam unsuitable due to too acidic

469 soils and steep slopes, whereas the local farmers can cultivate the land. Furthermore, the approach cannot account for
470 compound effects and interactions of the climate and soil variables (Elsheikh et al., 2013). The membership functions
471 cover the general behavior in a univariate manner, while the real plant physiology is a more complex interplay of climatic
472 variables and soil conditions (Joswig et al., 2022). This also applies particularly to compound extremes, for example the
473 combination of hot and dry climatic conditions (Goulart et al., 2023) that limit water availability and favor evaporation,
474 which can trigger water and temperature stress in plants. This is relevant in the course of a warming climate, as the joint
475 probability of hot and dry conditions is projected to increase in many regions of the world (Bevacqua et al., 2022; Felsche
476 et al., 2024). This is however no specific drawback of CropSuite, but rather a lack of bivariate, multivariate or interactive
477 membership functions. The assessment of the membership functions by Sys et al. (1993) is also outdated for new crop
478 varieties that might be more resilient to climatic and environmental stressors (Peter et al., 2020). Furthermore, we argue
479 that the uncertainty in the temperature and precipitation membership functions is by design larger at its low and high
480 ends, as the functions are derived empirically. Since our consideration of climate variability is based on the 5% to 10%
481 suitability values, respectively (see Section 2.2), the uncertainties of the membership functions are propagated to the
482 assessment of climate variability. More research and updated functions could support the results by CropSuite.
483 The sampling of climate variability within 20-year periods is limited as variability can cover wide time ranges. There,
484 the application of single-model initial condition large ensembles can help to robustly assess the variability based on
485 decadal or multidecadal time periods (Deser et al., 2020). This is especially important for precipitation and precipitation
486 extremes, which show a high sensitivity to climate variability (Lang and Poschlod, 2024; Tebaldi et al., 2021).
487 Furthermore, for the assessment of climate variability, we only capture the occurrence of growing seasons exceeding the
488 percentile thresholds, but we do not consider the intensity of the according events. Single days with extreme precipitation
489 can induce flooding that leads to crop failures (Balgah et al., 2023; Müller et al., 2023), even though the average
490 precipitation for the growing season is still within the suitable range of the membership function. This drawback however
491 also applies for most of the mechanistic crop models at global scale (Ruane et al., 2017), while regional applications
492 evolve incorporating crop losses due to waterlogging and flooding (Li et al., 2016; Monteleone et al., 2023; Pasley et al.,
493 2020). This is why we claim to assess climate variability not climate extremes inducing potential crop failures.

494 **6 Conclusions**

495 CropSuite is a new easy-to-use comprehensive open-source model that provides a complete processing chain
496 (preprocessing, spatial downscaling, suitability simulations, data analysis and visualization) for carrying out crop
497 suitability and climate change impact analysis. CropSuite allows users to easily parameterize different varieties of the
498 same crops or additional crops by determining the membership functions in the GUI. Thereby, the fuzzy logic approach
499 makes it easy to use expert knowledge for the parameterization of the membership functions. Besides all data and
500 compiled maps generated, we provide a user manual for CropSuite (Zabel and Knüttel, 2024) and the parameterizations

501 of the considered 48 crops in this study. Furthermore, the model allows the flexible addition of further parameters and
502 membership functions that might affect suitability, if the required data is provided. For the future, this allows the
503 consideration of further ecological and socio-economic limitations (such as access to fertilizers, available labor, know-
504 how, infrastructure and transportation, heat stress impacts on labor) that have not yet been sufficiently considered in crop
505 suitability assessments (Orlov et al., 2024; Akpoti et al., 2019).

506 For this study, we simulated 48 crops for Africa under the consideration of climate variability for historical climate
507 conditions. Thus, we created a huge dataset, providing detailed high-resolution information on climate-, soil-, and crop
508 suitability, optimal sowing dates, multiple cropping potentials and the limiting factors, which can be used for follow-up
509 studies and climate impact assessments. Additionally, the data include substantial information to develop strategies for
510 an efficient land-use (Schneider et al., 2024; Molina Bacca et al., 2023; Delzeit et al., 2019). The consideration of future
511 climate change scenarios will allow for investigating efficient strategies for climate change adaptation through shifting
512 sowing dates, or cultivar and land-use change. Further, information about the limiting factors can be helpful to optimize
513 crop management, since it identifies the parameter that most efficiently improves crop suitability.

514 **Code Availability**

515 CropSuite (v1.0) code is written in Python and is available Open-Source (CC BY-SA 4.0) together with the GUI at
516 Zenodo (<https://doi.org/10.5281/zenodo.14259375>) and GitHub (<https://github.com/flozabel/CropSuite>). A user manual
517 is provided separately via Zenodo (<https://doi.org/10.5281/zenodo.14196315>).

518 **Data Availability**

519 The resulting data are available for download as GeoTIFF files via Zenodo (<https://doi.org/10.5281/zenodo.14514729>).
520 In addition to the figures shown as examples for maize in this paper, the compiled figures for all 48 considered crops are
521 provided for download, including a separation of rainfed and irrigated agricultural systems and a comparison with
522 MapSPAM 2020 (<https://doi.org/10.5281/zenodo.14514729>).

523 **Author contribution**

524 FZ conceptualized and developed the model. MK programmed the CropSuite model and the GUI in Python. FZ, MK,
525 and BP developed the methodology for the consideration of climate variability. FZ and MK performed the simulations
526 and analyzed the results. FZ and MK prepared the manuscript with contributions from BP.

527 **Competing interests**

528 The authors declare that they have no conflict of interest.

529 **Acknowledgements**

530 The simulations were performed at sciCORE (<http://scicore.unibas.ch/>) scientific computing center at University of
531 Basel, requiring in total approximately 150.000 CPUh. We thank CGIAR and CIAT for their support and the scholarship
532 provided to MK and the collaboration for the Africa Agriculture Adaptation Atlas.

533 **References**

- 534 Abdulai, A. L., Kouressy, M., Vaksmann, M., Asch, F., Giese, M., and Holger, B.: Latitude and Date of Sowing
535 Influences Phenology of Photoperiod-Sensitive Sorghums, *Journal of Agronomy and Crop Science*, 198, 340-348,
536 10.1111/j.1439-037X.2012.00523.x, 2012.
- 537 Akpoti, K., Kabo-bah, A. T., and Zwart, S. J.: Review - Agricultural land suitability analysis: State-of-the-art and outlooks
538 for integration of climate change analysis, *Agricultural Systems*, 173, 172-208,
539 <https://doi.org/10.1016/j.agsy.2019.02.013>, 2019.
- 540 Akpoti, K., Kabo-bah, A. T., Dossou-Yovo, E. R., Groen, T. A., and Zwart, S. J.: Mapping suitability for rice production
541 in inland valley landscapes in Benin and Togo using environmental niche modeling, *Science of The Total
542 Environment*, 709, 136165, <https://doi.org/10.1016/j.scitotenv.2019.136165>, 2020.
- 543 Asseng, S., Spänkuch, D., Hernandez-Ochoa, I. M., and Laporta, J.: The upper temperature thresholds of life, *The Lancet
544 Planetary Health*, 5, e378-e385, [https://doi.org/10.1016/S2542-5196\(21\)00079-6](https://doi.org/10.1016/S2542-5196(21)00079-6), 2021.
- 545 Avellan, T., Zabel, F., and Mauser, W.: The influence of input data quality in determining areas suitable for crop growth
546 at the global scale – a comparative analysis of two soil and climate datasets, *Soil Use and Management*, 28, 249-265,
547 <https://doi.org/10.1111/j.1475-2743.2012.00400.x>, 2012.
- 548 Balgah, R. A., Ngwa, K. A., Buchenrieder, G. R., and Kimengsi, J. N.: Impacts of Floods on Agriculture-Dependent
549 Livelihoods in Sub-Saharan Africa: An Assessment from Multiple Geo-Ecological Zones, *Land*, 12, 334, 2023.
- 550 Batjes, N. H.: Harmonized soil property values for broad-scale modelling (WISE30sec) with estimates of global soil
551 carbon stocks, *Geoderma*, 269, 61-68, <https://doi.org/10.1016/j.geoderma.2016.01.034>, 2016.
- 552 Bevacqua, E., Zappa, G., Lehner, F., and Zscheischler, J.: Precipitation trends determine future occurrences of compound
553 hot-dry events, *Nat Clim Change*, 12, 350-355, 10.1038/s41558-022-01309-5, 2022.
- 554 Bonfante, A., Monaco, E., Alfieri, S. M., De Lorenzi, F., Manna, P., Basile, A., and Bouma, J.: Chapter Two - Climate
555 Change Effects on the Suitability of an Agricultural Area to Maize Cultivation: Application of a New Hybrid Land
556 Evaluation System, in: *Advances in Agronomy*, edited by: Sparks, D. L., Academic Press, 33-69,
557 <https://doi.org/10.1016/bs.agron.2015.05.001>, 2015.
- 558 Chapman, S., E Birch, C., Pope, E., Sallu, S., Bradshaw, C., Davie, J., and H Marsham, J.: Impact of climate change on
559 crop suitability in sub-Saharan Africa in parameterized and convection-permitting regional climate models,
560 *Environmental Research Letters*, 15, 094086, 10.1088/1748-9326/ab9daf, 2020.
- 561 Chemura, A., Gleixner, S., and Gornott, C.: Dataset of the suitability of major food crops in Africa under climate change,
562 *Scientific Data*, 11, 294, 10.1038/s41597-024-03118-1, 2024.
- 563 Chen, D., Dai, A., and Hall, A.: The Convective-To-Total Precipitation Ratio and the “Drizzling” Bias in Climate Models,
564 *Journal of Geophysical Research: Atmospheres*, 126, e2020JD034198, <https://doi.org/10.1029/2020JD034198>, 2021.
- 565 Cober, E. R. and Morrison, M. J.: Regulation of seed yield and agronomic characters by photoperiod sensitivity and
566 growth habit genes in soybean, *Theoretical and Applied Genetics*, 120, 1005-1012, 10.1007/s00122-009-1228-6,
567 2010.

568 Cronin, J., Zabel, F., Dessens, O., and Anandarajah, G.: Land suitability for energy crops under scenarios of climate
569 change and land-use, *GCB Bioenergy*, 12, 648–665-648–665, <https://doi.org/10.1111/gcbb.12697>, 2020.

570 Daly, C., Neilson, R. P., and Phillips, D. L.: A Statistical-Topographic Model for Mapping Climatological Precipitation
571 over Mountainous Terrain, *Journal of Applied Meteorology and Climatology*, 33, 140-158,
572 [https://doi.org/10.1175/1520-0450\(1994\)033<0140:ASTMFM>2.0.CO;2](https://doi.org/10.1175/1520-0450(1994)033<0140:ASTMFM>2.0.CO;2), 1994.

573 Damiani, A., Ishizaki, N. N., Sasaki, H., Feron, S., and Cordero, R. R.: Exploring super-resolution spatial downscaling
574 of several meteorological variables and potential applications for photovoltaic power, *Scientific Reports*, 14, 7254,
575 10.1038/s41598-024-57759-8, 2024.

576 Delzeit, R., Pongratz, J., Schneider, J. M., Schuenemann, F., Mauser, W., and Zabel, F.: Forest restoration: Expanding
577 agriculture, *Science*, 366, 316–317-316–317, <https://doi.org/10.1126/science.aaz0705>, 2019.

578 Deser, C., Lehner, F., Rodgers, K. B., Ault, T., Delworth, T. L., DiNezio, P. N., Fiore, A., Frankignoul, C., Fyfe, J. C.,
579 Horton, D. E., Kay, J. E., Knutti, R., Lovenduski, N. S., Marotzke, J., McKinnon, K. A., Minobe, S., Randerson, J.,
580 Screen, J. A., Simpson, I. R., and Ting, M.: Insights from Earth system model initial-condition large ensembles and
581 future prospects, *Nat Clim Change*, 10, 277-286, 10.1038/s41558-020-0731-2, 2020.

582 Dewitte, O., Jones, A., Spaargaren, O., Breuning-Madsen, H., Brossard, M., Dampha, A., Deckers, J., Gallali, T., Hallett,
583 S., Jones, R., Kilasara, M., Le Roux, P., Michéli, E., Montanarella, L., Thiombiano, L., Van Ranst, E., Yemefack, M.,
584 and Zougmore, R.: Harmonisation of the soil map of Africa at the continental scale, *Geoderma*, 211-212, 138-153,
585 <https://doi.org/10.1016/j.geoderma.2013.07.007>, 2013.

586 Dinku, T., Funk, C., Peterson, P., Maidment, R., Tadesse, T., Gadain, H., and Ceccato, P.: Validation of the CHIRPS
587 satellite rainfall estimates over eastern Africa, *Quarterly Journal of the Royal Meteorological Society*, 144, 292-312,
588 <https://doi.org/10.1002/qj.3244>, 2018.

589 Elsheikh, R., Mohamed Shariff, A. R. B., Amiri, F., Ahmad, N. B., Balasundram, S. K., and Soom, M. A. M.: Agriculture
590 Land Suitability Evaluator (ALSE): A decision and planning support tool for tropical and subtropical crops, *Comput*
591 *Electron Agr*, 93, 98-110, <https://doi.org/10.1016/j.compag.2013.02.003>, 2013.

592 FAO: The Ecocrop Database [dataset], 2024.

593 FAO, IIASA, ISRIC, ISSCAS, and JRC: Harmonized World Soil Database (version 1.2) [dataset], 2012.

594 Farr, T. G., Rosen, P. A., Caro, E., Crippen, R., Duren, R., Hensley, S., Kobrick, M., Paller, M., Rodriguez, E., Roth, L.,
595 Seal, D., Shaffer, S., Shimada, J., Umland, J., Werner, M., Oskin, M., Burbank, D., and Alsdorf, D.: The Shuttle
596 Radar Topography Mission, *Reviews of Geophysics*, 45, RG2004, 10.1029/2005RG000183, 2007.

597 Felsche, E., Böhnisch, A., Poschlod, B., and Ludwig, R.: European hot and dry summers are projected to become more
598 frequent and expand northwards, *Communications Earth & Environment*, 5, 410, 10.1038/s43247-024-01575-5,
599 2024.

600 Fick, S. E. and Hijmans, R. J.: WorldClim 2: new 1-km spatial resolution climate surfaces for global land areas,
601 *International Journal of Climatology*, 37, 4302-4315, 10.1002/joc.5086, 2017.

602 Fiddes, J., Aalstad, K., and Lehning, M.: TopoCLIM: rapid topography-based downscaling of regional climate model
603 output in complex terrain v1.1, *Geosci. Model Dev.*, 15, 1753-1768, 10.5194/gmd-15-1753-2022, 2022.

604 Fischer, G., Nachtergaele, F. O., van Velthuizen, H. T., Chiozza, F., Franceschini, G., Henry, M., Muchoney, D., and
605 Tramberend, S.: Global Agro-Ecological Zones v4 - Model documentation, 1, FAO, Rome,
606 <https://doi.org/10.4060/cb4744en>, 2021.

607 Franke, J. A., Müller, C., Minoli, S., Elliott, J., Folberth, C., Gardner, C., Hank, T., Izaurrealde, R. C., Jägermeyr, J., Jones,
608 C. D., Liu, W., Olin, S., Pugh, T. A. M., Ruane, A. C., Stephens, H., Zabel, F., and Moyer, E. J.: Agricultural
609 breadbaskets shift poleward given adaptive farmer behavior under climate change, *Global Change Biol*, 28, 167–181-
610 167–181, <https://doi.org/10.1111/gcb.15868>, 2021.

611 Funk, C., Peterson, P., Landsfeld, M., Pedreros, D., Verdin, J., Shukla, S., Husak, G., Rowland, J., Harrison, L., Hoell,
612 A., and Michaelsen, J.: The climate hazards infrared precipitation with stations—a new environmental record for
613 monitoring extremes, *Scientific Data*, 2, 150066, 10.1038/sdata.2015.66, 2015.

614 Funk, C., Peterson, P., Peterson, S., Shukla, S., Davenport, F., Michaelsen, J., Knapp, K. R., Landsfeld, M., Husak, G.,
615 Harrison, L., Rowland, J., Budde, M., Meiburg, A., Dinku, T., Pedreros, D., and Mata, N.: A High-Resolution 1983–
616 2016 Tmax Climate Data Record Based on Infrared Temperatures and Stations by the Climate Hazard Center, *Journal*
617 *of Climate*, 32, 5639-5658, <https://doi.org/10.1175/JCLI-D-18-0698.1>, 2019.

618 Gbode, I. E., Babalola, T. E., Diro, G. T., and Intsiful, J. D.: Assessment of ERA5 and ERA-Interim in Reproducing
619 Mean and Extreme Climates over West Africa, *Advances in Atmospheric Sciences*, 40, 570-586, 10.1007/s00376-
620 022-2161-8, 2023.

621 Gleixner, S., Demissie, T., and Diro, G. T.: Did ERA5 Improve Temperature and Precipitation Reanalysis over East
622 Africa?, *Atmosphere*, 11, 996, 2020.

623 Goulart, H. M. D., van der Wiel, K., Folberth, C., Balkovic, J., and van den Hurk, B.: Storylines of weather-induced crop
624 failure events under climate change, *Earth Syst. Dynam.*, 12, 1503-1527, 10.5194/esd-12-1503-2021, 2021.

625 Goulart, H. M. D., van der Wiel, K., Folberth, C., Boere, E., and van den Hurk, B.: Increase of Simultaneous Soybean
626 Failures Due To Climate Change, *Earth's Future*, 11, e2022EF003106, <https://doi.org/10.1029/2022EF003106>, 2023.

627 Hengl, T., de Jesus, J. M., MacMillan, R. A., Batjes, N. H., Heuvelink, G. B. M., Ribeiro, E., Samuel-Rosa, A., Kempen,
628 B., Leenaars, J. G. B., Walsh, M. G., and Gonzalez, M. R.: SoilGrids1km — Global Soil Information Based on
629 Automated Mapping, *PLOS ONE*, 9, e105992, 10.1371/journal.pone.0105992, 2014.

630 Hengl, T., Mendes de Jesus, J., Heuvelink, G. B. M., Ruiperez Gonzalez, M., Kilibarda, M., Blagotić, A., Shangguan,
631 W., Wright, M. N., Geng, X., Bauer-Marschallinger, B., Guevara, M. A., Vargas, R., MacMillan, R. A., Batjes, N.
632 H., Leenaars, J. G. B., Ribeiro, E., Wheeler, I., Mantel, S., and Kempen, B.: SoilGrids250m: Global gridded soil
633 information based on machine learning, *PLOS ONE*, 12, e0169748, 10.1371/journal.pone.0169748, 2017.

634 Hersbach, H., Bell, B., Berrisford, P., Hirahara, S., Horányi, A., Muñoz-Sabater, J., Nicolas, J., Peubey, C., Radu, R.,
635 Schepers, D., Simmons, A., Soci, C., Abdalla, S., Abellan, X., Balsamo, G., Bechtold, P., Biavati, G., Bidlot, J.,
636 Bonavita, M., De Chiara, G., Dahlgren, P., Dee, D., Diamantakis, M., Dragani, R., Flemming, J., Forbes, R., Fuentes,
637 M., Geer, A., Haimberger, L., Healy, S., Hogan, R. J., Hólm, E., Janisková, M., Keeley, S., Laloyaux, P., Lopez, P.,
638 Lupu, C., Radnoti, G., de Rosnay, P., Rozum, I., Vamborg, F., Villaume, S., and Thépaut, J.-N.: The ERA5 global
639 reanalysis, *Quarterly Journal of the Royal Meteorological Society*, 146, 1999-2049, <https://doi.org/10.1002/qj.3803>,
640 2020.

641 Herzberg, R., Pham, T. G., Kappas, M., Wyss, D., and Tran, C. T. M.: Multi-Criteria Decision Analysis for the Land
642 Evaluation of Potential Agricultural Land Use Types in a Hilly Area of Central Vietnam, *Land*, 8, 90, 2019.

643 IFPRI: Global Spatially-Disaggregated Crop Production Statistics Data for 2020 Version 1.0, Harvard Dataverse
644 [dataset], <https://doi.org/10.7910/DVN/SWPENT>, 2024.

645 IPCC: Climate Change 2021: The Physical Science Basis. Contribution of Working Group I to the Sixth Assessment
646 Report of the Intergovernmental Panel on Climate Change, Cambridge University Press, 2021.

647 Ivushkin, K., Bartholomeus, H., Bregt, A. K., Pulatov, A., Kempen, B., and de Sousa, L.: Global mapping of soil salinity
648 change, *Remote Sens Environ*, 231, 111260, <https://doi.org/10.1016/j.rse.2019.111260>, 2019.

649 Jägermeyr, J., Robock, A., Elliott, J., Müller, C., Xia, L., Khabarov, N., Folberth, C., Schmid, E., Liu, W., Zabel, F.,
650 Rabin, S. S., Puma, M. J., Heslin, A., Franke, J., Foster, I., Asseng, S., Bardeen, C. G., Toon, O. B., and Rosenzweig,
651 C.: A regional nuclear conflict would compromise global food security, *Proceedings of the National Academy of
652 Sciences*, 117, 7071–7081-7071–7081, <https://doi.org/10.1073/pnas.1919049117>, 2020.

653 Jägermeyr, J., Müller, C., Ruane, A. C., Elliott, J., Balkovic, J., Castillo, O., Faye, B., Foster, I., Folberth, C., Franke, J.
654 A., Fuchs, K., Guarin, J. R., Heinke, J., Hoogenboom, G., Iizumi, T., Jain, A. K., Kelly, D., Khabarov, N., Lange, S.,
655 Lin, T.-S., Liu, W., Mialyk, O., Minoli, S., Moyer, E. J., Okada, M., Phillips, M., Porter, C., Rabin, S. S., Scheer, C.,
656 Schneider, J. M., Schyns, J. F., Skalsky, R., Smerald, A., Stella, T., Stephens, H., Webber, H., Zabel, F., and
657 Rosenzweig, C.: Climate impacts on global agriculture emerge earlier in new generation of climate and crop models,
658 *Nature Food*, 2, 873–885-873–885, <https://doi.org/10.1038/s43016-021-00400-y>, 2021.

659 Joswig, J. S., Wirth, C., Schuman, M. C., Kattge, J., Reu, B., Wright, I. J., Sippel, S. D., Rieger, N., Richter, R.,
660 Schaepman, M. E., van Bodegom, P. M., Cornelissen, J. H. C., Diaz, S., Hattingh, W. N., Kramer, K., Lens, F.,
661 Niinemets, Ü., Reich, P. B., Reichstein, M., Römermann, C., Schrödt, F., Anand, M., Bahn, M., Byun, C., Campetella,
662 G., Cerabolini, B. E. L., Craine, J. M., Gonzalez-Melo, A., Gutiérrez, A. G., He, T., Higuchi, P., Jactel, H., Kraft, N.
663 J. B., Minden, V., Onipchenko, V., Peñuelas, J., Pillar, V. D., Sosinski, Ê., Soudzilovskaia, N. A., Weiher, E., and
664 Mahecha, M. D.: Climatic and soil factors explain the two-dimensional spectrum of global plant trait variation, *Nature
665 Ecology & Evolution*, 6, 36-50, 10.1038/s41559-021-01616-8, 2022.

666 Karger, D. N., Lange, S., Hari, C., Reyer, C. P. O., Conrad, O., Zimmermann, N. E., and Frieler, K.: CHELSA-W5E5:
667 daily 1 km meteorological forcing data for climate impact studies, *Earth Syst. Sci. Data*, 15, 2445-2464,
668 10.5194/essd-15-2445-2023, 2023.

669 Karl, K., MacCarthy, D., Porciello, J., Chimwaza, G., Fredenberg, E., Freduah, B. S., Guarin, J., Mendez Leal, E.,
670 Kozlowski, N., Narh, S., Sheikh, H., Valdivia, R., Wesley, G., Van Deynze, A., van Zonneveld, M., and Yang, M.:
671 Opportunity Crop Profiles for the Vision for Adapted Crops and Soils (VACS) in Africa,
672 <https://doi.org/10.7916/7msa-yy32>, 2024.

673 Knüttel, M. and Zabel, F.: CropSuite User Manual, <https://doi.org/10.5281/zenodo.14196315>, 2024.

674 Lang, A. and Poschlod, B.: Updating catastrophe models to today's climate – An application of a large ensemble approach
675 to extreme rainfall, *Climate Risk Management*, 44, 100594, <https://doi.org/10.1016/j.crm.2024.100594>, 2024.

676 Lemma, E., Upadhyaya, S., and Ramsankaran, R.: Investigating the performance of satellite and reanalysis rainfall
677 products at monthly timescales across different rainfall regimes of Ethiopia, *International Journal of Remote Sensing*,
678 40, 4019-4042, 10.1080/01431161.2018.1558373, 2019.

679 Li, S., Tompkins, A. M., Lin, E., and Ju, H.: Simulating the impact of flooding on wheat yield – Case study in East China,
680 *Agr Forest Meteorol*, 216, 221-231, <https://doi.org/10.1016/j.agrformet.2015.10.014>, 2016.

681 Maleki, F., Kazemi, H., Siahmarguee, A., and Kamkar, B.: Development of a land use suitability model for saffron
682 (*Crocus sativus* L.) cultivation by multi-criteria evaluation and spatial analysis, *Ecol Eng*, 106, 140-153,
683 <https://doi.org/10.1016/j.ecoleng.2017.05.050>, 2017.

684 Marke, T., Mauser, W., Pfeiffer, A., Zängl, G., Jacob, D., and Strasser, U.: Application of a hydrometeorological model
685 chain to investigate the effect of global boundaries and downscaling on simulated river discharge, *Environ Earth Sci*,
686 71, 4849-4868, 10.1007/s12665-013-2876-z, 2014.

687 Meier, J., Zabel, F., and Mauser, W.: A global approach to estimate irrigated areas – a comparison between different data
688 and statistics, *Hydrology and Earth System Sciences*, 22, 1119–1133-1119–1133, 2018.

689 Molina Bacca, E. J., Stevanović, M., Bodirsky, B. L., Karstens, K., Chen, D. M.-C., Leip, D., Müller, C., Minoli, S.,
690 Heinke, J., Jägermeyr, J., Folberth, C., Iizumi, T., Jain, A. K., Liu, W., Okada, M., Smerald, A., Zabel, F., Lotze-
691 Campen, H., and Popp, A.: Uncertainty in land-use adaptation persists despite crop model projections showing lower
692 impacts under high warming, *Communications Earth & Environment*, 4, 284, 10.1038/s43247-023-00941-z, 2023.

693 Monteleone, B., Giusti, R., Magnini, A., Arosio, M., Domeneghetti, A., Borzi, I., Petrucci, N., Castellarin, A.,
694 Bonaccorso, B., and Martina, M. L. V.: Estimations of Crop Losses Due to Flood Using Multiple Sources of
695 Information and Models: The Case Study of the Panaro River, *Water*, 15, 1980, 2023.

696 Müller, C., Ouédraogo, W. A., Schwarz, M., Barteit, S., and Sauerborn, R.: The effects of climate change-induced
697 flooding on harvest failure in Burkina Faso: case study, *Frontiers in Public Health*, 11, 10.3389/fpubh.2023.1166913,
698 2023.

699 Müller, C., Jägermeyr, J., Franke, J. A., Ruane, A. C., Balkovic, J., Ciais, P., Dury, M., Falloon, P., Folberth, C., Hank,
700 T., Hoffmann, M., Izaurrealde, R. C., Jacquemin, I., Khabarov, N., Liu, W., Olin, S., Pugh, T. A. M., Wang, X.,
701 Williams, K., Zabel, F., and Elliott, J. W.: Substantial Differences in Crop Yield Sensitivities Between Models Call
702 for Functionality-Based Model Evaluation, *Earth's Future*, 12, e2023EF003773,
703 <https://doi.org/10.1029/2023EF003773>, 2024.

704 Muthoni, F. K., Odongo, V. O., Ochieng, J., Mugalavai, E. M., Mourice, S. K., Hoesche-Zeledon, I., Mwila, M., and
705 Bekunda, M.: Long-term spatial-temporal trends and variability of rainfall over Eastern and Southern Africa,
706 *Theoretical and Applied Climatology*, 137, 1869-1882, 10.1007/s00704-018-2712-1, 2019.

707 Orlov, A., Jägermeyr, J., Müller, C., Daloz, A. S., Zabel, F., Minoli, S., Liu, W., Lin, T.-S., Jain, A. K., Folberth, C.,
708 Okada, M., Poschlod, B., Smerald, A., Schneider, J. M., and Sillmann, J.: Human heat stress could offset potential
709 economic benefits of CO2 fertilization in crop production under a high-emissions scenario, *One Earth*, 7, 1250-1265,
710 <https://doi.org/10.1016/j.oneear.2024.06.012>, 2024.

711 Pasley, H. R., Huber, I., Castellano, M. J., and Archontoulis, S. V.: Modeling Flood-Induced Stress in Soybeans, *Frontiers*
712 *in Plant Science*, 11, 10.3389/fpls.2020.00062, 2020.

713 Pelletier, J. D., Broxton, P. D., Hazenberg, P., Zeng, X., Troch, P. A., Niu, G.-Y., Williams, Z., Brunke, M. A., and
714 Gochis, D.: A gridded global data set of soil, intact regolith, and sedimentary deposit thicknesses for regional and

715 global land surface modeling, *Journal of Advances in Modeling Earth Systems*, 8, 41-65,
716 <https://doi.org/10.1002/2015MS000526>, 2016.

717 Peter, B. G., Messina, J. P., Lin, Z., and Snapp, S. S.: Crop climate suitability mapping on the cloud: a geovisualization
718 application for sustainable agriculture, *Scientific Reports*, 10, 15487, 10.1038/s41598-020-72384-x, 2020.

719 Ramirez-Villegas, J., Jarvis, A., and Läderach, P.: Empirical approaches for assessing impacts of climate change on
720 agriculture: The EcoCrop model and a case study with grain sorghum, *Agr Forest Meteorol*, 170, 67-78,
721 <https://doi.org/10.1016/j.agrformet.2011.09.005>, 2013.

722 Ranjitkar, S., Sujakhu, N. M., Merz, J., Kindt, R., Xu, J., Matin, M. A., Ali, M., and Zomer, R. J.: Suitability Analysis
723 and Projected Climate Change Impact on Banana and Coffee Production Zones in Nepal, *PLOS ONE*, 11, e0163916,
724 10.1371/journal.pone.0163916, 2016.

725 Ruane, A. C., Rosenzweig, C., Asseng, S., Boote, K. J., Elliott, J., Ewert, F., Jones, J. W., Martre, P., McDermid, S. P.,
726 Müller, C., Snyder, A., and Thorburn, P. J.: An AgMIP framework for improved agricultural representation in
727 integrated assessment models, *Environmental Research Letters*, 12, 125003, 10.1088/1748-9326/aa8da6, 2017.

728 Schneider, J. M., Zabel, F., and Mauser, W.: Global inventory of suitable, cultivable and available cropland under
729 different scenarios and policies, *Scientific Data*, 9, <https://doi.org/10.1038/s41597-022-01632-8>, 2022a.

730 Schneider, J. M., Zabel, F., and Mauser, W.: Global inventory of suitable, cultivable and available cropland under
731 different scenarios and policies, *Scientific Data*, 9, 527, 10.1038/s41597-022-01632-8, 2022b.

732 Schneider, J. M., Delzeit, R., Neumann, C., Heimann, T., Seppelt, R., Schuenemann, F., Söder, M., Mauser, W., and
733 Zabel, F.: Effects of profit-driven cropland expansion and conservation policies, *Nature Sustainability*, 7, 1335-1347,
734 10.1038/s41893-024-01410-x, 2024.

735 Steinkopf, J. and Engelbrecht, F.: Verification of ERA5 and ERA-Interim precipitation over Africa at intra-annual and
736 interannual timescales, *Atmospheric Research*, 280, 106427, <https://doi.org/10.1016/j.atmosres.2022.106427>, 2022.

737 Sun, Y., Solomon, S., Dai, A., and Portmann, R. W.: How Often Does It Rain?, *Journal of Climate*, 19, 916-934,
738 10.1175/jcli3672.1, 2006.

739 Sys, C. O., van Ranst, E., and Debaveye, J.: Land evaluation: Part II Methods in Land Evaluation, G.A.D.C, Brussels,
740 1991.

741 Sys, C. O., van Ranst, E., Debaveye, J., and Beernaert, F.: Land evaluation: Part III Crop requirements, G.A.D.C,
742 Brussels, 1993.

743 Tebaldi, C., Dorheim, K., Wehner, M., and Leung, R.: Extreme metrics from large ensembles: investigating the effects
744 of ensemble size on their estimates, *Earth Syst. Dynam.*, 12, 1427-1501, 10.5194/esd-12-1427-2021, 2021.

745 Terblanche, D., Lynch, A., Chen, Z., and Sinclair, S.: ERA5-Derived Precipitation: Insights from Historical Rainfall
746 Networks in Southern Africa, *Journal of Applied Meteorology and Climatology*, 61, 1473-1484,
747 <https://doi.org/10.1175/JAMC-D-21-0096.1>, 2022.

748 van Zonneveld, M., Kindt, R., McMullin, S., Achigan-Dako, E. G., N'Danikou, S., Hsieh, W.-h., Lin, Y.-r., and Dawson,
749 I. K.: Forgotten food crops in sub-Saharan Africa for healthy diets in a changing climate, *Proceedings of the National
750 Academy of Sciences*, 120, e2205794120, 10.1073/pnas.2205794120, 2023.

751 Verdin, A., Funk, C., Peterson, P., Landsfeld, M., Tuholske, C., and Grace, K.: Development and validation of the
752 CHIRTS-daily quasi-global high-resolution daily temperature data set, *Scientific Data*, 7, 303, 10.1038/s41597-020-
753 00643-7, 2020.

754 Vogel, E., Donat, M. G., Alexander, L. V., Meinshausen, M., Ray, D. K., Karoly, D., Meinshausen, N., and Frieler, K.:
755 The effects of climate extremes on global agricultural yields, *Environmental Research Letters*, 14, 054010,
756 10.1088/1748-9326/ab154b, 2019.

757 Wang, F., Tian, D., Lowe, L., Kalin, L., and Lehrter, J.: Deep Learning for Daily Precipitation and Temperature
758 Downscaling, *Water Resources Research*, 57, e2020WR029308, <https://doi.org/10.1029/2020WR029308>, 2021.

759 Yu, Q., You, L., Wood-Sichra, U., Ru, Y., Joglekar, A. K. B., Fritz, S., Xiong, W., Lu, M., Wu, W., and Yang, P.: A
760 cultivated planet in 2100 – Part 2: The global gridded agricultural-production maps, *Earth Syst. Sci. Data*, 12, 3545-
761 3572, 10.5194/essd-12-3545-2020, 2020.

762 Zabel, F.: Global Agricultural Land Resources – A High Resolution Suitability Evaluation and Its Perspectives until 2100
763 under Climate Change Conditions (v3.0) Zenodo [dataset], <https://doi.org/10.5281/zenodo.5982577>, 2022.

764 Zabel, F. and Knüttel, M.: CropSuite Version 1.0 User Manual, 21.05.2024.

765 Zabel, F., Putzenlechner, B., and Mauser, W.: Global Agricultural Land Resources – A High Resolution Suitability
766 Evaluation and Its Perspectives until 2100 under Climate Change Conditions, PLoS ONE, 9, e107522-e107522,
767 <https://doi.org/10.1371/journal.pone.0107522>, 2014.
768